SFB 649 Discussion Paper 2009-001

Implied Market Price of Weather Risk

Wolfgang Karl Härdle*
Brenda López Cabrera*

*Humboldt-Universität zu Berlin, Germany

This research was supported by the Deutsche Forschungsgemeinschaft through the SFB 649 "Economic Risk".

http://sfb649.wiwi.hu-berlin.de
ISSN 1860-5664

SFB 649, Humboldt-Universität zu Berlin
Spandauer Straße 1, D-10178 Berlin

Implied Market Price of Weather Risk

Wolfgang Karl Härdle, Brenda López Cabrera

CASE - Center for Applied Statistics and Economics
Humboldt-Universität zu Berlin

Abstract

Weather influences our daily lives and choices and has an enormous impact on corporate revenues and earnings. Weather derivatives differ from most derivatives in that the underlying weather cannot be traded and their market is relatively illiquid. The weather derivative market is therefore incomplete. This paper implements a pricing methodology for weather derivatives that can increase the precision of measuring weather risk. We have applied continous autoregressive models (CAR) with seasonal variation to model the temperature in Berlin and with that to get the explicite nature of non-arbitrage prices for temperature derivatives. We infer the implied market price from Berlin cumulative monthly temperature futures that are traded at the Chicago Mercantile Exchange (CME), which is an important parameter of the associated equivalent martingale measures used to price and hedge weather future/options in the market. We propose to study the market price of risk, not only as a piecewise constant linear function, but also as a time dependent object. In all of the previous cases, we found that the market price of weather risk is different from zero and shows a seasonal structure. With the extract information we price other exotic options, such as cooling/heating degree day temperatures and non-standard maturity contracts.

Keywords: Weather derivatives, weather risk, weather forecasting, seasonality, continuous autoregressive model, stochastic variance, CAT index, CDD index, HDD index, market price of risk, risk premium, CME

JEL classification: G19, G29, N26, N56, Q29, Q54

Acknowledgements: The financial support from the Deutsche Forschungsgemeinschaft via SFB 649 "Ökonomisches Risiko", Humboldt-Universität zu Berlin is gratefully acknowledged.

1 Introduction

Weather influences our daily lives and has an enormous impact on corporate revenues and earnings. The global climate changes the volatility of weather and the occurrence of extreme weather events increases. Adverse and extreme natural events like hurricanes, long cold winters, heat waves, droughts, freezes, etc. may cause substantial financial losses. The traditional way of protection against unpredictable weather conditions has always been the insurance, which covers the loss in exchange for the payment of a premium. However, recently

have become popular new financial instruments linked to weather conditions: CAT bonds, sidecars and weather derivatives.

In the 1990's Weather Derivatives (WD) were developed to hedge against volatility caused by weather. WD are financial contracts, where payments are based on weather-related measurements. They are formally exchanged in the Chicago Mercantile Exchange (CME), where monthly and seasonal temperature futures, call and put options contracts on future prices are traded. The futures and options at the CME are cash settled. WD cover against extreme changes in temperature, rainfall, wind, snow, frost, but do not cover catastrophic events, such as hurricanes. According to the CME (2006), the WD market increased notably from 2.2 billion USD in 2004 to 22 billion USD through to September 2005.

The key factor in efficient usage of WD is a reliable valuation procedure. However, due to their specific nature one encounters several difficulties. Firstly, weather derivatives are different from most financial derivatives because the underlying weather cannot be traded. Secondly, the weather derivatives market is relatively illiquid, i.e. weather derivatives cannot be cost-efficiently replicated by other weather derivatives.

In practice, the valuation of WD is in spirit and methodolgy closer to insurance pricing than to derivative pricing (arbitrage pricing) since their value is equal to the expected outcome under the physical probability plus a charge depending on a risk measure (usually the standard deviation), Jewson, Brix and Ziehmann (2005).

The pricing of weather derivatives has attracted the attention of many researchers. Dornier and Querel (2000) fitted an Ornstein-Uhlenbeck stochastic process with constant variance to temperature observations at Chicago O'Hare airport and started to investigate future prices on temperature indices. Later Alaton, Djehiche and Stillberger (2002) applied the Ornstein-Uhlenbeck model with a monthly variation in the variance to temperature data of Bromma airport (Stockholm). They applied their model to get prices for different temperature prices. Campbell and Diebold (2005) modelled temperature in several US cities with a higher order autoregressive model. They observed seasonal behaviour in the autocorrelation function (ACF) of the squared residuals. However, they did not price temperature derivatives. Mraoua and Bari (2007) studied the temperature in Casablanca, Morocco using a mean reverting model with stochastic volatility and a temperature swap was considered. Benth (2003) calculates an arbitrage free price for different temperature derivatives prices by using the fractional Brownian motion model of Brody, Syroka and Zervos (2002), which drives the noise in an Ornstein-Uhlenbeck process.

In the temperature derivative market, Davis (2001) proposed using a marginal utility technique to price temperature derivatives based on the HDD index. Barrieu and El Karoui (2002) present an optimal design of weather derivatives in an illiquid framework, arguing that the standard risk neutral point of view is not applicable to valuate them. Cao and Wei (2004) and Richards, Manfredo and Sanders (2004) apply an extended version of Lucas' (1978) equilibrium pricing model where direct estimation of market price of weather risk is avoided. Instead, pricing is based on the stochastic processes of the weather index, an aggregated dividend and an assumption about the utility function of a representative investor. Platen and West (2005) used the world stock

index as the numeraire to price temperature derivatives. Benth and Saltyte Benth (2005) and (2007) propose the continuous time autoregressive model with seasonality for the temperature evolution in time and match this model to data observed in Stockholm, Sweden. They derive future and option prices for contracts on CDD and CAT indices. They also discuss hedging strategies for the options and the volatility term structure. For pricing a New York WD, **?** carried out an empirical study for the New York over the counter (OTC) future prices and other weather contracts to extract the risk neutral distribution and the market price of weather risk. Hung-Hsi, Yung-Ming and Pei-Syun (2008) extended the long term temperature model proposed by Alaton et al. (2002) by taking into account ARCH/GARCH effects to reflect the clustering of volatility temperature. They examine the effects of mean, variance and market price of risk on HDD/CDD option prices and demonstrate that their effects are similar to those on the prices of traditional options.

In this paper, we apply continous autoregressive models (CAR) with seasonal variation to model the temperature in Berlin, as Benth, Koekebakker and Saltyte Benth (2007) did for Stockholm Temperature data in order to get the explicite nature of non-arbitrage prices for temperature derivatives. In contrast to this work we find that Berlin Temperature is more normal in the sense that the driving stochastics are closer to a Wiener Process than their analysis for Stockholm. The estimate of the market price of weather risk (MPR) is interesting by its own and has not been studied earlier. The MPR adjusts the underlying process so that the level of the risk aversion is not needed for valuation. The majority of papers so far have solved it assuming zero MPR, but this assumption underestimates WD prices. By using the theoretical explicit prices we imply the market price of temperature risk for Berlin futures. We find that the market price of risk is different from zero. We show the seasonal structure when the MPR is assumed to be piecewise constant linear function or time dependent. Not only, the MPR estimate is important for pricing derivatives (future/options) but also for hedging and for pricing new non-standard contracts with "non-standard maturities" and other OTC contracts. By using the implied MPR from Berlin Cumulative Average Temperature (CAT) futures, we price new derivatives, e.g. Cold Degree Days (CDD) and Heating Degree Days (HDD) for Berlin. A clear seasonal variation in the regression residuals of the temperature is observed and the volatility term structure of CAT temperature futures presents a modified Samuelson effect.

Our paper is structured as follows. The next section - the econometric part - is devoted to explaining the dynamics of Berlin temperature data by using a continous autoregressive model (CAR). In section 3, we discuss the fundamentals of temperature derivatives (future and options), their indices and we also describe the monthly temperature futures traded at CME, the biggest market offering this kind of product. In section 4, the financial mathematics part of the paper is explained by the connection of the weather with pricing dynamics. We imply the market price of risk for Berlin monthly temperature futures which are traded at the Chicago Mercantile Exchange (CME). We study the market price of risk, not only as a piecewise constant linear function, but also as time dependent for different contract types. In any of the previous cases, we found that the market price of weather risk is different from zero and shows a seasonal structure. With the extract information we price other exotic options, such as cooling/heating degree day temperatures and non-standard maturity contracts. Section 5 concludes the paper. All computations in this paper were carried out in Matlab version 7.6.

2 Berlin temperature dynamics

In this section, we study the weather dynamics for Berlin daily temperature data. The temperature data was obtained from the Deutscher Wetterdienst. It considers 22063 recordings of daily average temperatures from 19500101-20080527 at Tempelhof Airport Weather Station.

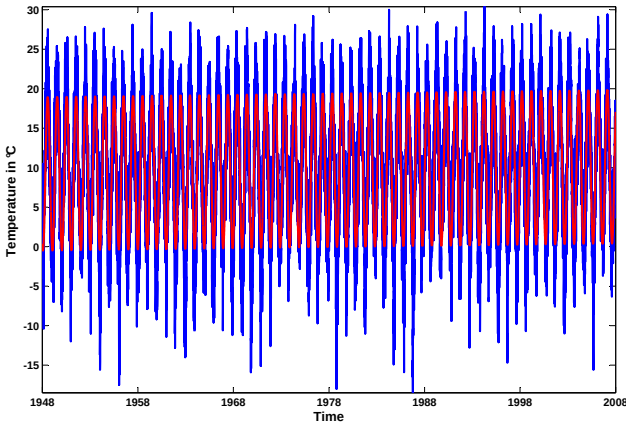

Figure 1: Seasonality effect (red line) and daily average temperatures 19480101-20080527, Tempelhof Airport Weather Station.

We first check the presence of a linear trend and investigate the seasonal pattern of the data. A linear trend was not detectable. Figure 1 shows 57 years of daily average temperature from Berlin and the least squares fitted seasonal function with trend

$$\Lambda_t = a_0 + a_1 t + a_2 cos\left\{\frac{2\pi(t-a_3)}{365}\right\} \tag{1}$$

where $\hat{a}_0 = 91.52, \hat{a}_1 = 0.00, \hat{a}_2 = 97.96, \hat{a}_3 = -165.1$ with 95% confidence bounds and R^2 equal to 0.7672. In Figure 2 we display, for better exposition, a stretch of 8.5 years. We observe low temperatures in the winter and high temperatures in the summer.

After removing the seasonality (equation 1) from the daily average temperatures,

$$X_t = T_t - \Lambda_t \tag{2}$$

we check whether X_t is a stationary process $I(0)$. In order to do that, we apply the Augmented Dickey-Fuller test (ADF):

$$(1-L)X_t = c_1 + \mu t + \tau LX + \alpha_1(1-L)LX_t + \ldots \alpha_p(1-L)L^pX_t + \varepsilon_t$$

where p is the number of lags of X_t by which the regression is augmented to get residuals free of autocorrelation. Under H_0 (unit root), τ should be zero. Therefore the test statistic of the OLS estimator of τ is applicable. In this case, $\tau = -35.001$ with 1% critical value equal to -2.56. We reject the null hypothesis H_0 ($\tau = 0$) and hence X_t is a stationary process $I(0)$. This result can also be verified by using the KPSS Test:

$$X_t = c + \mu t + k\sum_{i=1}^{t}\xi_i + \varepsilon_t$$

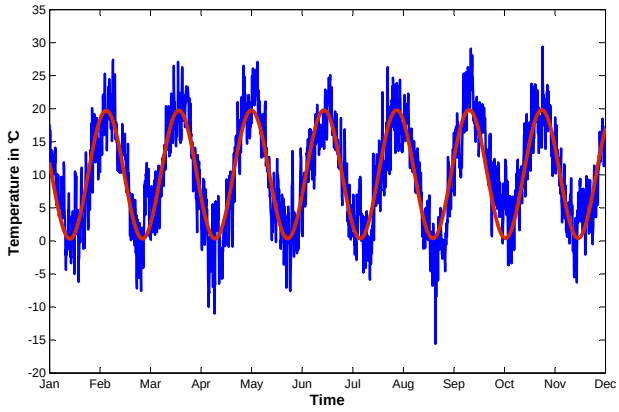

Figure 2: Seasonality effect (red line) and daily average temperature from Berlin 2000101-20080527, Tempelhof Airport Weather Station.

We accept $H_0 : k = 0$ at 10% significance level that the process is stationary. The test statistic for the constant is equal to 0.653 and for the trend equal to 0.139.

The Partial Autocorrelation Function (PACF) of Equation 2 is plotted in Figure 3. The PACF suggests that the AR(3) model suggested by Benth et al. (2007) also holds for Berlin temperature data. $p = 3$ is also confirmed by the log of Akaike's Final Prediction Error. The fitted autoregressive process is equal to:

$$X_{t+3} = 0.91X_{t+2} - 0.20X_{t+1} + 0.08X_t + \sigma_t\varepsilon_t \tag{3}$$

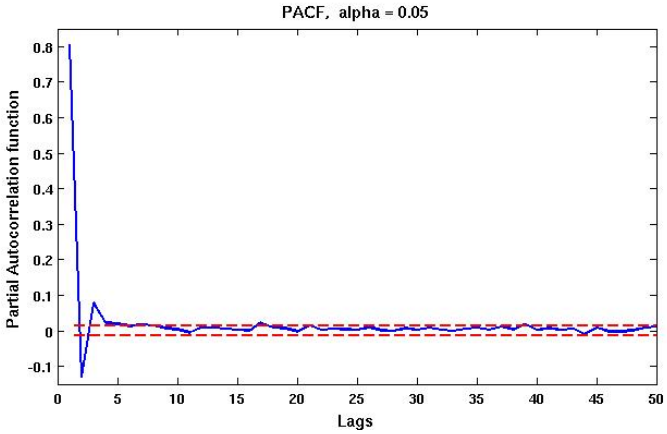

Figure 3: Partial autocorrelation function (PACF) for X_t 19480101-20080527

After trend and seasonal components were removed, the residuals ε_t and the squared residuals ε_t^2 of the Berlin temperature data of equation 3 are plotted in Figure 4. According to the modified Li-McLeod Portmanteau test, we reject at 0% significance level the null hypothesis H_0 that the residuals are uncorrelated. The ACF of the residuals of AR(3), upper panel in Figure 5, is close to zero and according to Box-Ljung statistic the first

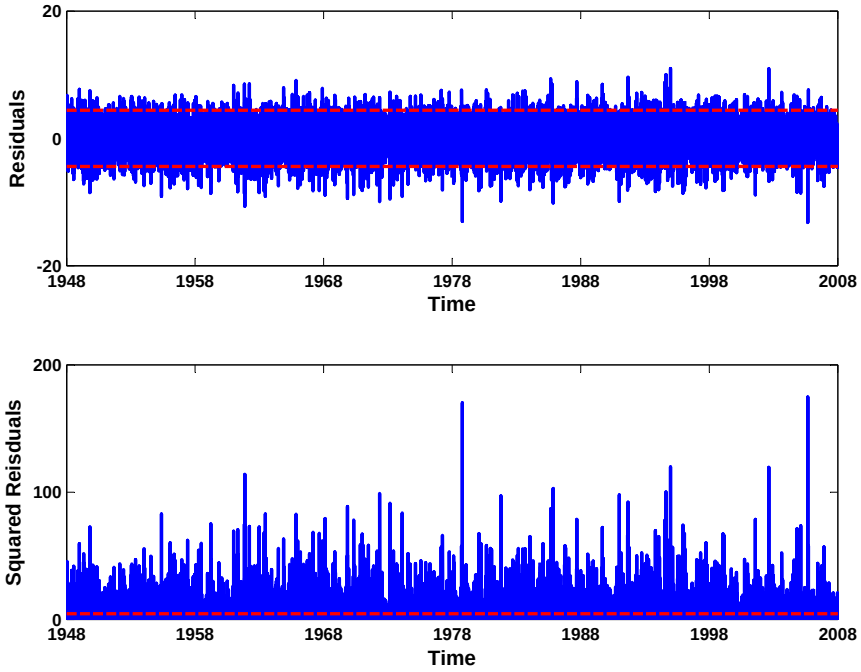

Figure 4: Residuals $\hat{\varepsilon}_t$ (up) and squared residuals $\hat{\varepsilon}_t^2$ (down) of the AR(3) during 19480101-20080527

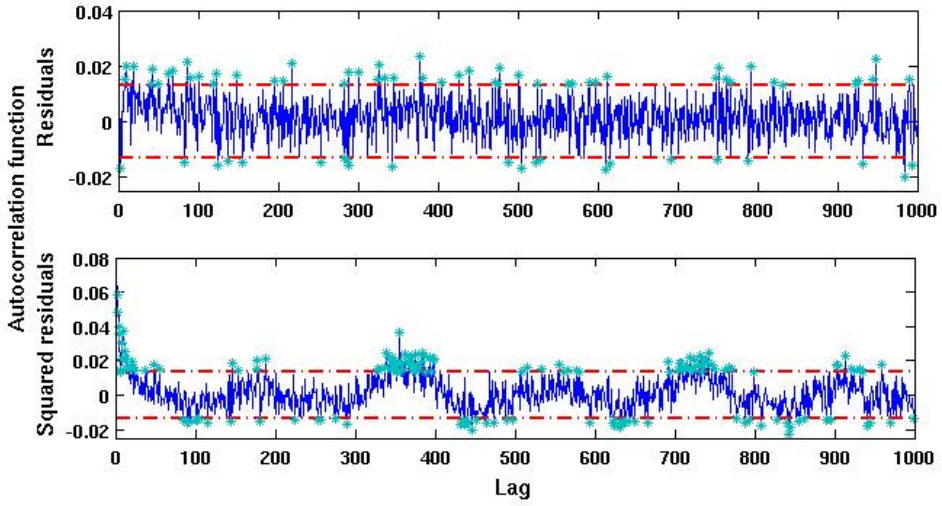

Figure 5: ACF for residuals $\hat{\varepsilon}_t$ (up) and squared residuals $\hat{\varepsilon}_t^2$ (down) of the AR(3) during 19480101-20080527

few lags are insignificant. But, the ACF for the squared residuals in the lower panel in Figure 5 shows a high seasonality pattern. We calibrate this seasonal dependence of variance of residuals of the AR(3) for 57 years with a truncanted Fourier function

$$\sigma_t^2 = c_1 + \sum_{i=1}^{4} \left\{ c_{2i} \cos\left(\frac{2i\pi t}{365}\right) + c_{2i+1} \sin\left(\frac{2i\pi t}{365}\right) \right\} \tag{4}$$

Alternatively one could have smoothed the data with a kernel regression estimator. Asympotically they can be approximated by Fourier series estimators though. Figure 6 shows the daily empirical variance (the average of squared residuals for each day of the year) and the fitted squared volatility function for the residuals. Here we obtain the Campbell and Diebold (2005) effect for Stockholm temperature data, high variance in winter - earlier summer and low variance in spring - late summer. Figure 7 shows the Berlin temperature residuals $\hat{\varepsilon}_t$ and squared residuals $\hat{\varepsilon}_t^2$, after dividing out the seasonal volatility σ_t from the regression residuals, we observed close to normal residuals. The ACF plot of the residuals remain unchanged and now the ACF plot for squared residuals presents a non-seasonal pattern, Figure 8.

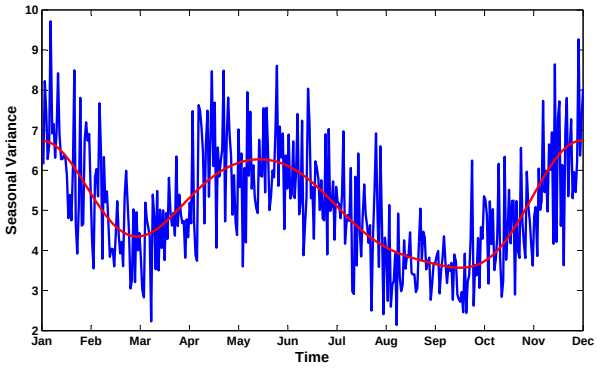

Figure 6: Seasonal variance: daily empirical variance (blue line), fitted squared volatility function (red line) at 10% significance level. $\hat{c}_1 = 5.09$, $\hat{c}_2 = 0.64$, $\hat{c}_3 = 0.74$, $\hat{c}_4 = 0.95$, $\hat{c}_5 = -0.45$, $\hat{c}_6 = 0.44$, $\hat{c}_7 = 0.05$, $\hat{c}_8 = 0.81$, $\hat{c}_9 = 0.81$

Table 1 presents the statistics and the corresponding significance levels of the lags of the ACF of residuals with and without seasonal volatility. The Ljung-Box's test statistic (Qstat) is used to check the significance level of the lags.

The Kernel smoothing density estimate against a Normal Kernel evaluated at 100 equally spaced points for Berlin temperature residuals in the left hand side of Figure 9 has been plotted to verify if residuals become normally distributed. The obtained residuals have a skewness equal to -0.08,a kurtosis equal to 3.56 and Jarques Bera statistics equal to 318.96. The acceptance of the null hyptohesis H_0 of normality is at 1% significance level. The right hand side of Figure 9 shows the log of the estimated distribution function.

The q'th coordinate of vector $\mathbf{X}$ with $q = 1, .., p$, X_q from the temperature time series:

$$T_t = \Lambda_t + X_{1t} \tag{5}$$

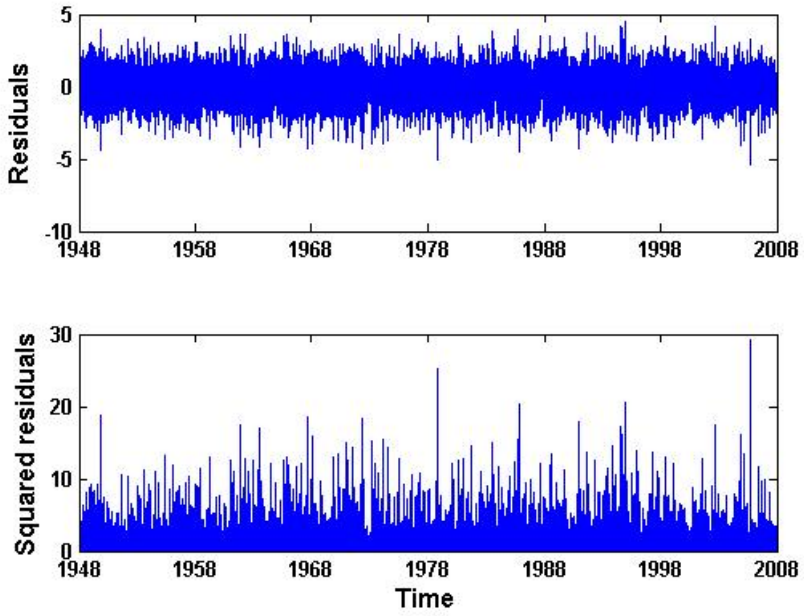

Figure 7: Berlin temperature residuals $\hat{\varepsilon}_t$ (up) and squared residuals $\hat{\varepsilon}_t^2$ (down) after correcting for seasonal volatility

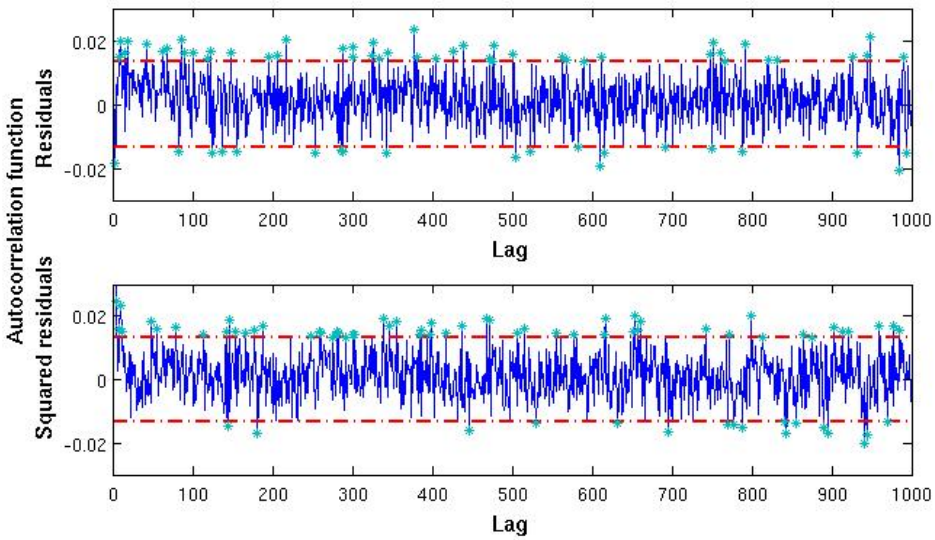

Figure 8: ACF for Berlin temperature residuals $\hat{\varepsilon}_t$ (up) and squared residuals $\hat{\varepsilon}_t^2$ (down) after correcting for seasonal volatility

Lag	$Qstat_{res}$	$QSIG_{res}$	$Qstat_{res1}$	$QSIG_{res1}$
1	0.03	0.85	0.67	0.41
2	0.05	0.97	0.74	0.69
3	3.16	0.36	4.88	0.18
4	4.70	0.32	6.26	0.18
5	4.76	0.44	6.67	0.24
6	5.40	0.49	7.17	0.30
7	6.54	0.47	7.51	0.37
8	10.30	0.24	10.34	0.24
9	14.44	0.10	14.65	0.10
10	21.58	0.01	21.95	0.10

Table 1: Q-test (Qstat) using Ljung-Box's and the corresponding significance levels (QSIG) for residuals with (res) and without seasonality in the variance (res1)

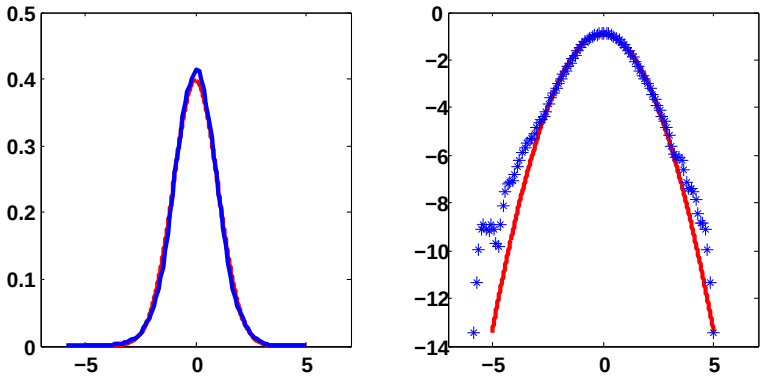

Figure 9: Left: Kernel smoothing density estimate (blue line) vs Normal Kernel (red line) for Berlin temperature residuals. Right: Kernel smoothing density estimate (blue line) vs Logormal Kernel (red line) for Berlin temperature residuals

can be seen as a discretization of a continuous-time process AR(p) ($CAR(p)$) and can be specified as a Markov process. Define a $p \times p$-matrix:

$$A = \begin{pmatrix} 0 & 1 & 0 & \dots & 0 & 0 \\ 0 & 0 & 1 & \dots & 0 & 0 \\ \vdots & & \ddots & & 0 & \vdots \\ 0 & \dots & \dots & 0 & 0 & 1 \\ -\alpha_p & -\alpha_{p-1} & \dots & & 0 & -\alpha_1 \end{pmatrix} \tag{6}$$

in the vectorial Ornstein-Uhlenbleck process $\mathbf{X}_t \in \mathbb{R}^p$ for $p \geq 1$ as:

$$d\mathbf{X}_t = A\mathbf{X}_t dt + \mathbf{e}_{pt}\sigma_t dB_t \tag{7}$$

where $\mathbf{e}_k$ denotes the k'th unit vector in $\mathbb{R}^p$ for $k = 1, ...p$, $\sigma_t > 0$ states the temperature volatility, B_t is a Wiener Process and α_k are positive constants.

By applying the multidimensional *Itô Formula*, the process 7 with $\mathbf{X}_t = \mathbf{x} \in \mathbb{R}^p$ has the explicit form:

$$\mathbf{X}_s = \exp\{A(s-t)\}\mathbf{x} + \int_t^s \exp\{A(s-u)\}\mathbf{e}_p\sigma_u dB_u \tag{8}$$

for $s \geq t \geq 0$ and stationarity holds when the eigenvalues of A have negative real part or the variance matrix

$$\int_0^t \sigma_{t-s}^2 \exp\{A(s)\}\mathbf{e}_p\mathbf{e}_p^\top \exp\left\{A^\top(s)\right\} ds \tag{9}$$

converges as $t \to \infty$.

By substituting iteratively into the discrete-time dynamics, one obtains the discrete version of the $CAR(p)$ process 7. For example, when $p = 1, 2, 3$ and using $\varepsilon_t = B_{t+1} - B_t$, we repeat the exercise:

for $p = 1$, we get that $\mathbf{X}_t = X_{1t}$ and $dX_{1t} = -\alpha_1 X_{1t}dt + \sigma_t dB_t$.
for $p = 2$, we have:

$$X_{1(t+2)} \approx (2 - \alpha_1)X_{1(t+1)} + (\alpha_1 - \alpha_2 - 1)X_{1(t)} + \sigma_t(B_{t-1} - B_t)$$

for $p = 3$, the iterations yield:

$$\begin{aligned}
X_{1(t+1)} - X_{1(t)} &= X_{1(t)}dt + \sigma_t\varepsilon_t \\
X_{2(t+1)} - X_{2(t)} &= X_{3(t)}dt + \sigma_t\varepsilon_t \\
X_{3(t+1)} - X_{3(t)} &= -\alpha_3 X_{1(t)}dt - \alpha_2 X_{2(t)}dt - \alpha_1 X_{3(t)}dt + \sigma_t\varepsilon_t \\
X_{1(t+2)} - X_{1(t+1)} &= X_{1(t+1)}dt + \sigma_{t+1}\varepsilon_{t+1} \\
X_{2(t+2)} - X_{2(t+1)} &= X_{3(t+1)}dt + \sigma_{t+1}\varepsilon_{t+1} \\
X_{3(t+2)} - X_{3(t+1)} &= -\alpha_3 X_{1(t+1)}dt - \alpha_2 X_{2(t+1)}dt - \alpha_1 X_{3(t+1)}dt + \sigma_{t+1}\varepsilon_{t+1} \qquad (10) \\
X_{1(t+3)} - X_{1(t+2)} &= X_{1(t+2)}dt + \sigma_{t+2}\varepsilon_{t+2} \\
X_{2(t+3)} - X_{2(t+2)} &= X_{3(t+2)}dt + \sigma_{t+2}\varepsilon_{t+2} \\
X_{3(t+3)} - X_{3(t+2)} &= -\alpha_3 X_{1(t+2)}dt - \alpha_2 X_{2(t+2)}dt - \alpha_1 X_{3(t+2)}dt + \sigma_{t+2}\varepsilon_{t+2}
\end{aligned}$$

(11)

substituting into the X_1 dynamics:

$$\begin{aligned} X_{1(t+3)} &\approx (3-\alpha_1)X_{1(t+2)} + (2\alpha_1 - \alpha_2 - 3)X_{1(t+1)} + (-\alpha_1 + \alpha_2 - \alpha_3 + 1)X_{1(t)} \\ &+ \sigma_t(B_{t-1} - B_t) \end{aligned} \tag{12}$$

For Berlin temperature we have identified $p = 3$, see Figure 3. The AR(3) is equal to $X_{t+3} = 0.91X_{t+2} - 0.20X_{t+1} + 0.07X_t + \sigma_t\varepsilon_t$. The $CAR(3)$-parameters are therefore $\alpha_1 = 2.09, \alpha_2 = 1.38, \alpha_3 = 0.22$. The stationarity condition is fulfilled, since the eigenvalues of A have negative real parts ($\lambda_1 = -0.2069, \lambda_{2,3} = -0.9359 \pm 0.3116i$). The element components of the matrix A do not change over time, this makes the process stable.

3 A pricing model

In this section we describe the construction of pricing Future/Option for different temperature contracts.

3.1 Temperature derivatives

Temperature derivatives are written on a temperature index. The most common weather indices on temperature are: Heating Degree Day (HDD), Cooling Degree Day (CDD), Cumulative Averages (CAT), Average of Average Temperature (AAT) and Event Indices (EI), Jewson et al. (2005). The HDD index measures the temperature over a period $[\tau_1, \tau_2]$, usually between October to April, and it is defined as:

$$HDD(\tau_1, \tau_2) = \int_{\tau_1}^{\tau_2} \max(c - T_u, 0)du \tag{13}$$

where c is the baseline temperature (typically 18C or 65F) and T_u is the average temperature on day u. Similarly, the CDD index measures the temperature over a period $[\tau_1, \tau_2]$, usually between November and March, and it is defined as:

$$CDD(\tau_1, \tau_2) = \int_{\tau_1}^{\tau_2} \max(T_u - c, 0)du \tag{14}$$

The HDD and the CDD index are used to trade futures and options in 18 US cities (Atlanta, Des Moines, New York, Baltimore, Detroit, Philadelphia, Boston, Houston, Portland, Chicago, Kansas City, Sacramento, Cincinnati, Las Vegas, Salt Lake City, Dallas, Minneapolis-St. Paul, Tucson), six Canadian cities (Calgary, Edmonton, Montreal, Toronto, Vancouver and Winnipeg), nine European cities (Amsterdam, Essen, Paris, Barcelona, London, Rome, Berlin, Madrid, Stockholm) and two Japanese cities (Tokio and Osaka). The CAT index accounts the accumulated average temperature over a period $[\tau_1, \tau_2]$ days:

$$CAT(\tau_1, \tau_2) = \int_{\tau_1}^{\tau_2} T_u du \tag{15}$$

Since $\max(T_u - k, 0) - \max(K - T_u, 0) = T_u - k$, we get the HDD-CDD parity

$$CDD(\tau_1, \tau_2) - HDD(\tau_1, \tau_2) = CAT(\tau_1, \tau_2) - c(\tau_2 - \tau_1) \tag{16}$$

Indices	*Jan*	*Feb*	*March*	*April*	*May*	*Jun*	*Jul*	*Aug*	*Sept*	*Oct*	*Nov*	*Dec*
CDD	0	0	0	0	28.3	42	71	23.3	24.9	0	0	0
HDD	472.8	526.4	471.4	241.1	150.2	71.8	24.8	43.9	73.5	199.5	398.2	525.8
CAT	103.2	-4.4	104.6	316.9	454.1	528.2	622.2	555.4	509.4	376.5	159.8	50.2
AAT	3.32	-0.15	3.37	10.56	14.64	17.60	20.07	17.91	16.98	12.14	5.32	1.61

Table 2: Degree day indices for temperature data (2005) Berlin.

Therefore, it is sufficient to analyse only CDD and CAT indices. The AAT measures the "*excess*" or deficit of temperature i.e. the average of average temperatures over $[\tau_1, \tau_2]$ days:

$$AAT(\tau_1, \tau_2) = \frac{1}{\tau_1 - \tau_2} \int_{\tau_1}^{\tau_2} T_u du \tag{17}$$

This index is just the average of the CAT and it is relevant for the Pacific Rim consisting of two Japanese cities (Tokyo and Osaka). The event index (EI) considers the number of times a certain meteorological event occurs in the contract period. For example, a frosty day is considered when the temperature at 7:00-10:00 hrs local time is less than or equal to -3.5C. To illustrate this, Table 2 shows the number of HDDs, CDDs, CATs and AATs estimated by the Earth Satellite Corporation (the weather analysis provider of CME) and for the historical Berlin temperature data.

In this paper, we will focus on the pricing of some of the most common temperature futures traded at the CME, i.e. monthly CAT, CDD and HDD indices. Table 3 describes the CME - WD data from 20031003 - 20070521. The contract size of a future traded at CME is 20 pounds times the Degree Day Index (for convenience, we call it "price"). The minimum price increment is one Degree Day Index point. The degree day metric is Celsius and the tick value is twenty pounds. The termination of the trading is two calendar days following the expiration of the contract month. The Settlement is based on the relevant Degree Day index on the first exchange business day at least two calendar days after the futures contract month. The accumulation period of each CAT index futures contract begins with the first calendar day of the contract month and ends with the calendar day of the contract month. Earth Satellite Corporation reports to CME the daily average temperature. Traders bet that the temperature will not exceed the estimates from Earth Satellite Corporation. The notation used by CME for temperature futures is the following: F for January, G for February, H for March, J for April, K for May, M for June, N for July, Q for August, U for September, V for November and X for December. J7 stands for 2007, J8 for 2008, etc. The J7 contract corresponds to the month of April, i.e. with the temperature measurement period from 20070401 (τ_1) to 20070430 (τ_2) and trading period from 20060503 to 20070502. Figure 10 plots the values of Berlin monthly CAT and HDD Future Prices traded on 20060530 at the CME. Observe that seven contracts are traded for CAT futures (from April to October) and for HDD futures (from November to April). At the trading day t, one can buy contracts with measurement period $\tau_1 \leq t \leq \tau_2$ or $t < \tau_1 \leq \tau_2$ (six months ahead from the trading day t). Figure 11 shows the plot of Berlin CAT future prices from 20060501 to 20060530: future prices shown constant behaviour over the measurement period, but they increase when the temperature is high e.g. prices decrease from September to April.

To proceed with a correct estimation of the indices, we compare the plots of the Berlin CAT and HDD future

Trading-Period			Measurement-Period	
Code	First-trade	Last-trade	τ_1	τ_2
J7	20060503	20070502	20070401	20070430
K7	20060603	20070602	20070501	20070531
M7	20060705	20070702	20070601	20070630
N7	20060803	20070802	20070701	20070731
Q7	20060906	20070904	20070801	20070831
U7	20061003	20071002	20070901	20070930
V7	20061103	20071102	20071001	20071031
X7	20061204	20071202	20071101	20071130
Z7	20070104	20080102	20071201	20071231
F8	20080204	20080202	20080101	20080131
G8	20070304	20080302	20070201	20080228
H8	20070404	20080402	20070301	20080331

Table 3: Contracts listed at the CME. Source: Bloomberg

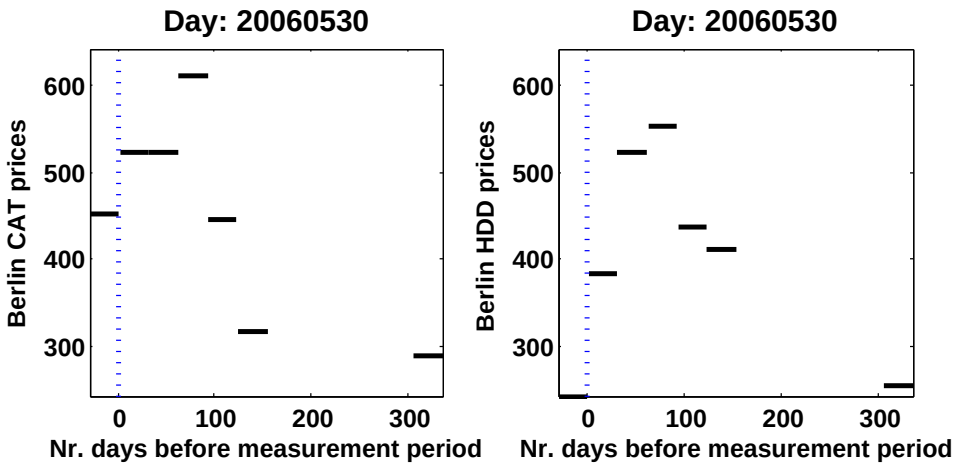

Figure 10: Berlin CAT (left side) - HDD (right side) Monthly Future Prices traded on 20060530 at the CME. Source: Bloomberg

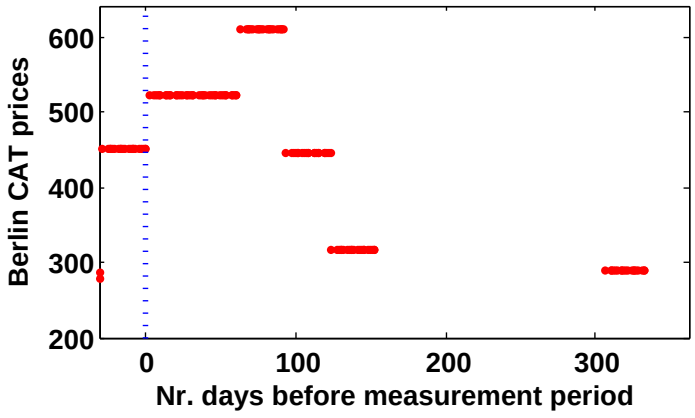

Figure 11: Berlin CAT Future Prices traded on 20060501-20060530 at the CME. Source: Bloomberg

prices with $\tau_1 < t \leq \tau_2$ from the period 2001 to 2006 reported by Bloomberg (red line), Earth Satellite Corporation (blue) and our estimates (black line) in Figure 12. The average relative difference from the values reported from Bloomberg and Earth Satellite Corporation is equal to 2.43 for HDD prices and -10.57 for CAT prices, while for our estimates and the values reported by Earth Satellite Corporation is equal to 0.04 and -0.09 respectively. This confirms that our temperature data is adequate to price temperature derivatives.

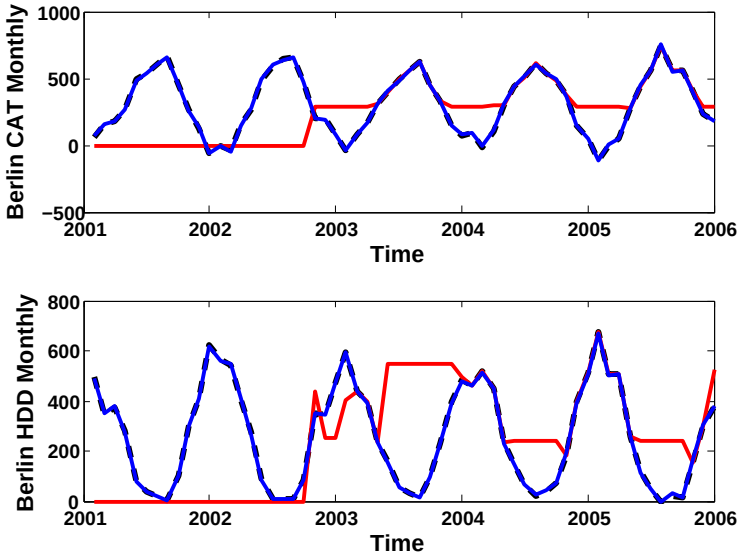

Figure 12: Berlin CAT (upper side) HDD (lower side) Future Prices estimated by the Earth Satellite Corporation (blue line) and from historical data (black line). Source: Bloomberg

3.2 Temperature futures pricing

As temperature is not a tradable asset in the market place, no replication arguments hold for any temperature futures and incompleteness of the market follows. In this context all equivalent measures Q will be risk-neutral probabilities. We assume the existance of a pricing measure Q, which can be parametrized and complete the market, Karatzas and Shreve (2001). For that, we pin down an equivalent measure $Q = Q_{\theta_t}$ to compute the arbitrage free price of a temperature future:

$$F_{(t,\tau_1,\tau_2)} = \mathrm{E}^{Q_{\theta_t}}\left[Y_T(T_t)|\mathcal{F}_t\right] \tag{18}$$

with $0 \leq t \leq T$ and Y_T being the payoff from the temperature index (CAT,HDD,CDD indices) at $T > t$ and θ_t denotes the time dependent market price of risk (MPR). By Girsanov theorem:

$$B_t^{\theta} = B_t - \int_0^t \theta_u du$$

is a Brownian motion for any time before the end of the trading time, i.e. $t \leq \tau_{\max}$ and a martingale under Q_{θ_t}. Here the market price of risk (MPR) θ_t is as a real valued, bounded and piecewise continous function. We later relax that assumption, by considering the (non)-time dependent market price of risk. In fact, from Theorem

4.2 (page 12) in Karatzas and Shreve (2001), we can parametrize the market price of risk θ_t and relate it to the risk premium for traded assets by the equation

$$\mu_t + \delta_t - r_t\tilde{1} = \sigma_t\theta_t \tag{19}$$

where $\tilde{1}$ denotes the N-dimensional vector with every component equal to one, μ_t is the N-dimensional mean rate of return process, δ_t defines a N-dimensional dividend rate process, σ_t denotes the volatility process and r_t determines the risk-free interest rate process of the traded asset. For example, in the Black-Scholes Model framework, the asset price follows:

$$S_t = S_0 \exp\left[\left\{\mu(S_t,t) - \frac{1}{2}\sigma^2(S_t,t)\right\}t + \sigma(S_t,t)B_t\right]$$

with $\frac{dS_t}{S_t} = \mu(S_t,t)dt + \sigma(S_t,t)dB_t$, where $t \in [0,T]$, B_t is standard Brownian motion under measure Q and by Girsanov theorem $B_t^\theta = B_t - \int_0^t \theta_u du = B_t - \int_0^t \left(\frac{\mu_u - r_u}{\sigma_u}\right) du$ is also Brownian motion under Q_{θ_t} for $t \leq \tau_{\max}$. Then, under Q_{θ_t}, the dynamics of the underlying process in the Black&Scholes framework are:

$$\frac{dS_t}{S_t} = \{\mu(S_t,t) + \sigma(S_t,t)\theta_t\}\,dt + \sigma(S_t,t)dB_t^\theta$$

Similarly, under Q^θ, the temperature dynamics of equation(8) become

$$d\mathbf{X}_t = (A\mathbf{X}_t + \mathbf{e}_p\sigma_t\theta_t)dt + \mathbf{e}_p\sigma_t dB_t^\theta \tag{20}$$

with explicit dynamics, for $s \geq t \geq 0$:

$$\mathbf{X}_s = \exp\{A(s-t)\}\mathbf{x} + \int_t^s \exp\{A(s-u)\}\mathbf{e}_p\sigma_u\theta_u du + \int_t^s \exp\{A(s-u)\}\mathbf{e}_p\sigma_u dB_u^\theta \tag{21}$$

Observe that the volatility σ_t from the econometric part is deterministic for every t, so that the relationship between θ_t and σ_t is well identified and can be compared to the Black&Scholes MPR for traded assets $\theta_t = (\mu_t - r_t)/\sigma_t$, meaning that the MPR of temperature futures is nothing other than the temperature variation σ_t.

3.2.1 CAT Futures

Following equation (18), the risk neutral price of a future based on a CAT index is defined as:

$$F_{CAT(t,\tau_1,\tau_2)} = \mathrm{E}^{Q_\theta}\left[\int_{\tau_1}^{\tau_2} T_s ds|\mathcal{F}_t\right] \tag{22}$$

For contracts whose trading date is earlier than the temperature measurement period, i.e. $0 \leq t \leq \tau_1 < \tau_2$, Benth et al. (2007) calculate the future price explicitly by inserting the temperature model (equation 5) into equation 22:

$$F_{CAT(t,\tau_1,\tau_2)} = \int_{\tau_1}^{\tau_2} \Lambda_u du + \mathbf{a}_{t,\tau_1,\tau_2}\mathbf{X}_t + \int_t^{\tau_1} \theta_u\sigma_u\mathbf{a}_{t,\tau_1,\tau_2}\mathbf{e}_p du + \int_{\tau_1}^{\tau_2} \theta_u\sigma_u\mathbf{e}_1^\top A^{-1}\left[\exp\{A(\tau_2-u)\} - I_p\right]\mathbf{e}_p du \tag{23}$$

with $\mathbf{a}_{t,\tau_1,\tau_2} = \mathbf{e}_1^\top A^{-1}\left[\exp\{A(\tau_2-t)\} - \exp\{A(\tau_1-t)\}\right]$ and $p \times p$ identity matrix $\mathtt{I}_p$.

We observed from real data that CME trades CAT futures between the temperature measurement period, i.e. $\tau_1 \leq t \leq \tau_2$. Following the same pricing methodology as before, we calculate the risk neutral price for these kind of contracts:

$$\begin{aligned} F_{CAT}(t,\tau_1,\tau_2) &= \mathrm{E}^{Q^\theta}\left[\int_{\tau_1}^{t} T_s ds|\mathcal{F}_t)\right] + \mathrm{E}^{Q^\theta}\left[\int_{t}^{\tau_2} T_s ds|\mathcal{F}_t\right] \\ &= \mathrm{E}^{Q^\theta}\left[\int_{\tau_1}^{t} T_s ds|\mathcal{F}_t\right] + \int_{t}^{\tau_2} \Lambda_u du + \mathbf{a}_{t,\tau_1,\tau_2}\mathbf{X}_t + \int_{t}^{\tau_2} \theta_u \sigma_u \mathbf{e}_1^\top A^{-1}\left[\exp\left\{A(\tau_2-u)\right\} - I_p\right]\mathbf{e}_p du \end{aligned}$$

where $\mathbf{a}_{t,t,\tau_2} = \mathbf{e}_1^\top A^{-1}\left[\exp\left\{A(\tau_2 - t)\right\} - I_p\right]$. Notice that this time the price of the future CAT consists on a random and deterministic part since the expected value of the temperature from τ_1 to t is known.

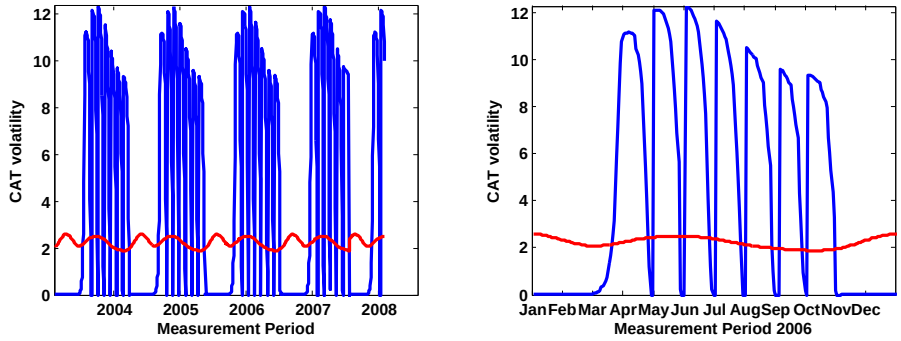

Figure 13: The Berlin CAT term structure of volatility from 2004-2008 (left) and 2006 (right) for contracts traded within the measurement period

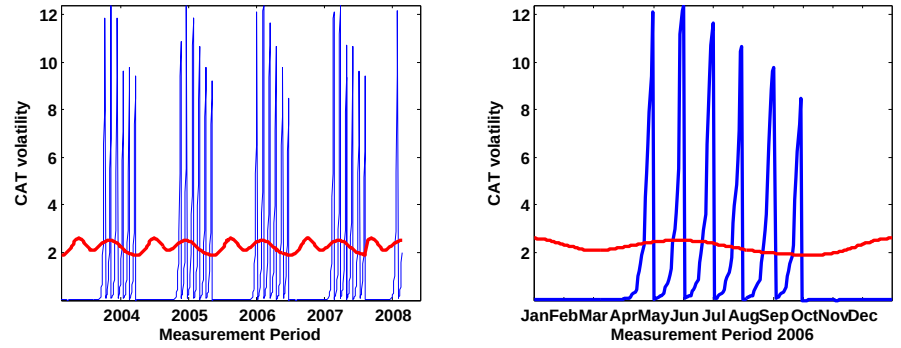

Figure 14: The Berlin CAT term structure of volatility from 2004-2008 (left) and 2006 (right) for contracts traded before the measurement period

For contracts traded within the measurement period, CAT volatility $\sigma_t \mathbf{a}_{t,\tau_1,\tau_2}\mathbf{e}_p$ is close to zero when the time to measurement is large. It decreases up to the end of the measurement period, since information about the temperature development is already known. On the left hand side of Figure 13 we plot the CAT volatility path for contracts issued within measurement periods in 2004-2008 and on the right hand side we display the plot for 2006. For contracts which were issued before the measurement period, we also observe a CAT future volatility close to zero when time to measurement is large, (temperature deviations are smoothed over time), however it increases up to the start of the measurement period. Figure 14 shows this effect for contracts issued before the

measurement period. In the literature, an effect of this nature is called Samuelson effect and it is very common in future contracts based on mean reverting commodity prices.

In Figure 15 we plot 2 contracts issued on 20060517: one with measurement period the first week of June and the other one as the whole month of June. The contract with the longest measurement period has the largest volatility. In contrast to the later effect, one can observe the effect of the $CAR(3)$ in both contracts when the volatility decays just before maturity of the contracts. These two effects observed on Berlin CAT futures are also similar for Stockholm CAT futures, Benth et al. (2007), however the deviations are less smoothed for Berlin.

3.2.2 CDD Futures

Analogously, one derives the CDD future price. Following equation (18), the risk neutral price of a CDD future which is traded at $0 \leq t \leq \tau_1 < \tau_2$ is defined as:

$$\begin{aligned} F_{CDD(t,\tau_1,\tau_2)} &= \mathrm{E}^{Q_\theta}\left[\int_{\tau_1}^{\tau_2} \max(T_s - c, 0) ds | \mathcal{F}_t\right] \\ &= \int_{\tau_1}^{\tau_2} \upsilon_{t,s} \psi\left[\frac{m_{\left\{t,s,\mathbf{e}_1^\top \exp\{A(s-t)\}\mathbf{X}_t\right\}} - c}{\upsilon_{t,s}}\right] ds \end{aligned} \tag{24}$$

where $m_{\{t,s,x\}} = \Lambda_s - c + \int_t^s \sigma_u \theta_u \mathbf{e}_1^\top \exp\{A(s-t)\}\mathbf{e}_p du + x$, $\upsilon_{t,s}^2 = \int_t^s \sigma_u^2 \left[\mathbf{e}_1^\top \exp\{A(s-t)\}\mathbf{e}_p\right]^2 du$ and $\psi(x) = x\Phi(x) + \varphi(x)$ with $x = \mathbf{e}_1^\top \exp\{A(s-t)\}\mathbf{X}_t$.

For CDD futures contracts traded at $\tau_1 \leq t \leq \tau_2$, the non-abitrage price of a CDD future is:

$$\begin{aligned} F_{CDD(t,\tau_1,\tau_2)} &= \mathrm{E}^{Q_\theta}\left[\int_{\tau_1}^{\tau_2} \max(T_s - c, 0) ds | \mathcal{F}_t\right] \\ &= \mathrm{E}^{Q_\theta}\left[\int_{\tau_1}^{t} \max(T_s - c, 0) ds | \mathcal{F}_t\right] + \int_t^{\tau_2} \upsilon_{t,s} \psi\left[\frac{m_{\left\{t,s,\mathbf{e}_1^\top \exp\{A(s-t)\}\mathbf{X}_t\right\}} - c}{\upsilon_{t,s}}\right] ds \end{aligned} \tag{25}$$

with $m_{\{t,s,x\}}$ and $\upsilon_{t,s}^2$ defined as above. Notice again that the expected value of the temperature from τ_1 to t is known.

4 Infering the market price of temperature risk

The incompleteness of the WD market, since weather is not a tradable asset, requires the estimation of the market price of weather risk (MPR) for pricing and hedging temperature derivatives. The MPR adjusts the underlying process so that one may perform correct and the level of risk aversion is not needed for valuation. In this part of the paper, we infer the market price of risk θ_t from Berlin monthly CAT temperature futures. Once we know the MPR for temperature futures, then we know the MPR for options. Moreover with this inferred information, we can price new derivatives, e.g. non-standard contracts with "non-standard maturities". We first study the contracts which are traded before the measurement period, i.e. $t < \tau_1 \leq \tau_2$ (or contract number

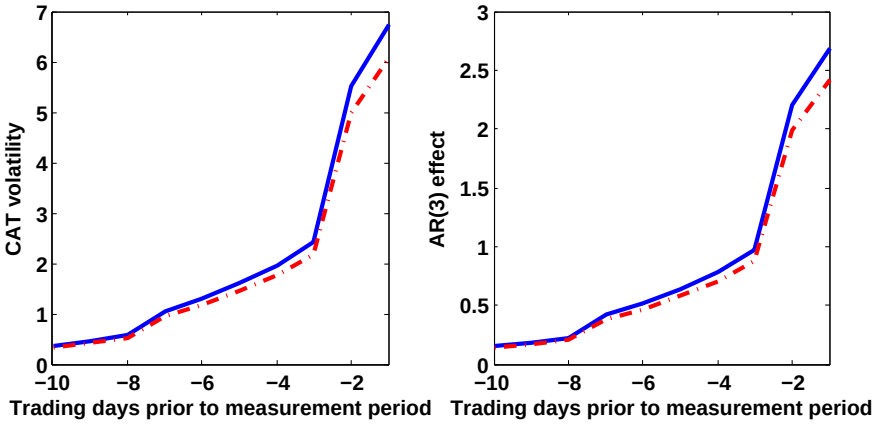

Figure 15: Berlin CAT volatility and AR(3) effect of 2 contracts issued on 20060517: one with whole of June as measurement period (blue line) and the other one with only the first week of June (red line)

$i = 2 \dots 7$), since their pricing value depends only on the expected value of the underlying process, while for the other contracts traded during the measurement period, i.e. $\tau_1 < t \leq \tau_2$ (or contract number $i = 1$), a partial or full information of the temperature development inside the measurement period is already known. Then, we mix both cases to study the dynamics of the MPR, when it is assumed to be piecewise constant or time dependent.

4.1 Constant market price of risk for each contract per trading day

From equation (23), we can infer θ_t for contracts with trading date $t < \tau_1 \leq \tau_2$. Our first assumption is to set $\hat{\theta}_t^i$ as a constant for each of the i contract, with $i = 2 \dots 7$. $\hat{\theta}_t^i$ is estimated via:

$$\begin{aligned} \underset{\hat{\theta}_t^i}{\arg\min} \quad \Bigg(& F_{CAT(t,\tau_1^i,\tau_2^i)} - \int_{\tau_1^i}^{\tau_2^i} \hat{\Lambda}_u du - \hat{\mathbf{a}}_{t,\tau_1^i,\tau_2^i} \mathbf{X}_t - \hat{\theta}_t^i \left\{ \int_t^{\tau_1} \hat{\sigma}_u \hat{\mathbf{a}}_{t,\tau_1^i,\tau_2^i} \mathbf{e}_p du \right. \\ & + \left. \int_{\tau_1^i}^{\tau_2^i} \hat{\sigma}_u \mathbf{e}_1^\top A^{-1} \left[\exp\left\{ A(\tau_2^i - u) \right\} - I_p \right] \mathbf{e}_p du \right\} \Bigg)^2 \end{aligned} \tag{26}$$

The right upper part of Figure 19 shows the MPR estimates for each contract per trading day for Berlin CAT Future Prices traded on 20060530. We reject $H_0 : E(\hat{\theta}) = 0$ under the Wald statistic $\left\{ \theta_t \in \mathbb{R}^6 \right\}_{t=1}^{1000}$: 0.087 with probability 0.2322.

4.2 Constant market price of risk per trading day

A simpler parametrization of θ_t is to assume that it is constant for all maturities. We therefore estimate this constant θ_t for all contracts with $t < \tau_1 \leq \tau_2$ as follows:

$$\begin{aligned} \underset{\hat{\theta}_t}{\arg\min}\, \Sigma_{i=2}^{7} \quad \Bigg(\quad & F_{CAT(t,\tau_1^i,\tau_2^i)} - \int_{\tau_1^i}^{\tau_2^i} \hat{\Lambda}_u du - \hat{\mathbf{a}}_{t,\tau_1^i,\tau_2^i} \mathbf{X}_t - \hat{\theta}_t \left\{ \int_t^{\tau_1^i} \hat{\sigma}_u \hat{\mathbf{a}}_{t,\tau_1^i,\tau_2^i} \mathbf{e}_p du \right. \\ + \quad & \left. \left. \int_{\tau_1^i}^{\tau_2^i} \hat{\sigma}_u \mathbf{e}_1^\top A^{-1} \left[\exp\left\{ A(\tau_2^i - u) \right\} - I_p \right] \mathbf{e}_p du \right\} \Bigg)^2 \end{aligned} \tag{27}$$

The corresponding picture to this parametrization is displayed in Figure 16. As we observed, this is a very robust estimation. We reject $H_0 : E(\hat{\theta}) = 0$ under the Wald statistic $\left\{\theta_t \in \mathbb{R}^6\right\}_{t=1}^{1000}$: 0.8066 with probability 0.6309.

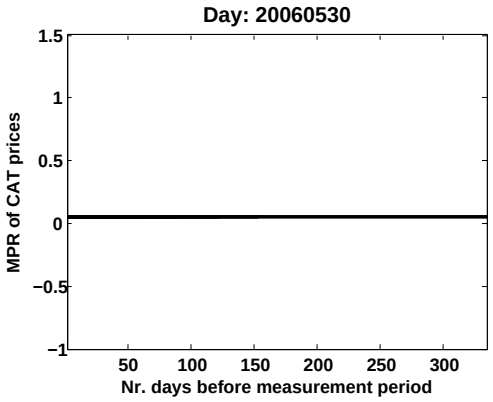

Figure 16: Constant MPR per trading day for Berlin CAT Futures traded on 20060530

4.3 Two constant market prices of risk per trading day

Assuming now that, instead of one constant market price of risk per trading day, we have a step function with jump $\hat{\theta}_t = I\left(u \leq \xi\right) \hat{\theta}_t^1 + I\left(u > \xi\right) \hat{\theta}_t^2$ with jump point ξ (take e.g. the first 150 days before the beginning of the measurement period). Then we estimate $\hat{\theta}_t$ by:

$$\begin{aligned} f(\xi) \quad = \quad & \underset{\hat{\theta}_t^1, \hat{\theta}_t^2}{\arg\min}\, \Sigma_{i=2}^{7} \Bigg(F_{CAT(t,\tau_1^i,\tau_2^i)} - \int_{\tau_1^i}^{\tau_2^i} \hat{\Lambda}_u du - \hat{\mathbf{a}}_{t,\tau_1^i,\tau_2^i} \mathbf{X}_t \\ - \quad & \hat{\theta}_t^1 \left\{ \int_t^{\tau_1^i} I\left(u \leq \xi\right) \hat{\sigma}_u \hat{\mathbf{a}}_{t,\tau_1^i,\tau_2^i} \mathbf{e}_p du + \int_{\tau_1^i}^{\tau_2^i} I\left(u \leq \xi\right) \hat{\sigma}_u \mathbf{e}_1^\top A^{-1} \left[\exp\left\{ A(\tau_2^i - u) \right\} - I_p \right] \mathbf{e}_p du \right\} \\ - \quad & \hat{\theta}_t^2 \left\{ \int_t^{\tau_1^i} I\left(u > \xi\right) \hat{\sigma}_u \hat{\mathbf{a}}_{t,\tau_1^i,\tau_2^i} \mathbf{e}_p du + \int_{\tau_1^i}^{\tau_2^i} I\left(u > \xi\right) \hat{\sigma}_u \mathbf{e}_1^\top A^{-1} \left[\exp\left\{ A(\tau_2^i - u) \right\} - I_p \right] \mathbf{e}_p du \right\} \Bigg)^2 \end{aligned} \tag{28}$$

The lower left part of Figure 19 shows the MPR estimates with $\xi = 150$ days for Berlin CAT Future Prices traded on 20060530. We notice that the value of the MPR decreases when the value of ξ increases, i.e. when

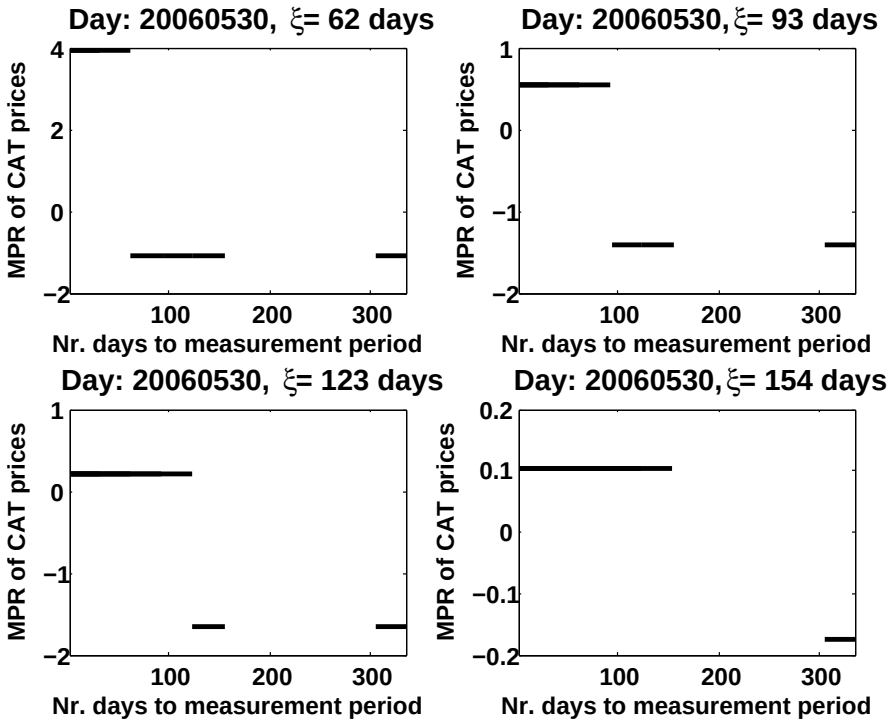

Figure 17: Two constant MPRs with $\xi = 62, 93, 123, 154$ days (upper left, upper right, lower left, lower right) for contracts with trading day 20060530 before the measurement period

the time to measurement period gets large. This effect is related to the Samuelson effect, where the volatility for each contract is close to zero when the time to measurement period is large. In a next step we optimized the value of ξ, it was choosen such as $f(\xi)$ in equation 28 is minimized. For $\xi = 62, 93, 123, 154$ days, the corresponding sum of squared errors are 2759, 14794, 15191 and 15526. Figure 17 shows the MPR estimates for different values of ξ of Berlin CAT Future Prices traded on 20060530, a date before the measurement period. The line is broken for those days when there is no trading of such contracts. Figure 18 shows the same situation as before but now all kinds of contracts are considered, i.e. sold contracts during and before the measurement period. We reject $H_0 : E(\hat{\theta}) = 0$ under the Wald statistic $\left\{\theta_t \in \mathbb{R}^6\right\}_{t=1}^{1000}$: 0.8005 with a probability of 0.058.

4.4 General form of the market price of risk per trading day

Generalising the piecewise continuous function given in the previous subsection, the (inverse) problem of determining θ_t can be formulated via a series expansion for θ_t:

$$\begin{aligned}\underset{\hat{\gamma}_k}{\arg\min}\, \Sigma_{i=2}^{7} \quad \Bigg(\quad & F_{CAT(t,\tau_1^i,\tau_2^i)} - \int_{\tau_1^i}^{\tau_2^i} \hat{\Lambda}_u du - \hat{\mathbf{a}}_{t,\tau_{1^i},\tau_2^i} \hat{\mathbf{X}}_t - \int_t^{\tau_1^i} \sum_{k=1}^{K} \hat{\gamma}_k \hat{h}_k(u_i) \hat{\sigma}_{u_i} \hat{\mathbf{a}}_{t,\tau_1,\tau_2} \mathbf{e}_p du_i \\ - \quad & \int_{\tau_1^i}^{\tau_2^i} \sum_{k=1}^{K} \hat{\gamma}_k \hat{h}_k(u_i) \hat{\sigma}_{u_i} \mathbf{e}_1^\top A^{-1} \left[\exp\left\{A(\tau_2^i - u_i)\right\} - I_p\right] \mathbf{e}_p du_i \Bigg)^2 \end{aligned} \tag{29}$$

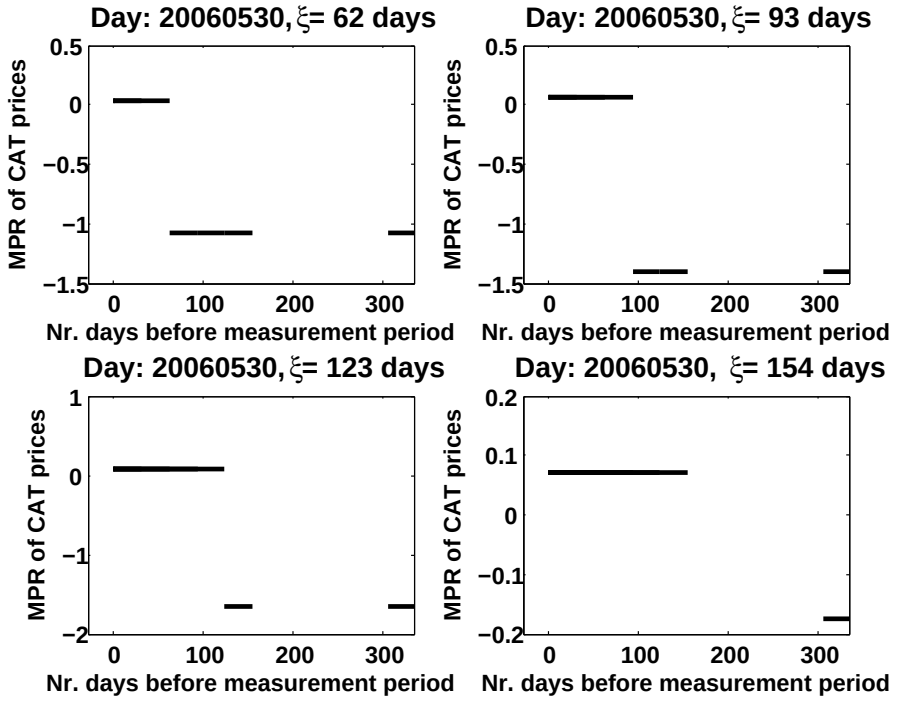

Figure 18: Two constant MPRs with $\xi = 62, 93, 123, 154$ days (upper left, upper right, lower left, lower right) for contracts with trading day 20060530 in and before the measurement period

where $h_k(u_i)$ is a vector of known basis functions and γ_k defines the coefficients. Here $h_k(u_i)$ may denote a spline basis for example. The right lower part of Figure 19 shows the MPR per trading day for Berlin CAT Future Prices traded on 20060530 using cubic polynomios with number of knots equal to the number of traded contracts (6). The spline MPR is closed to zero, but then it explodes for the days when there is no trading.

4.5 Bootstrapping market price of risk

The bootstrap method can be applied to get estimates of the MPR for contracts with a trading date earlier than the measurement period. If six contracts are traded at a time $t < \tau_1^i \leq \tau_2^i$ with $i = 2 \dots 7$ and $\tau_1^i < \tau_1^{i+1} \leq \tau_2^i < \tau_2^{i+1}$, the resampling idea method consists on the estimation of $\hat{\theta}_2$ from the second contract ($i = 2$):

$$\begin{aligned} \underset{\hat{\theta}_t^2}{\arg\min} \quad \Bigg(& F_{CAT(t,\tau_1^2,\tau_2^2)} - \int_{\tau_1^2}^{\tau_1^2} \hat{\Lambda}_u du - \hat{\mathbf{a}}_{t,\tau_1^2,\tau_2^2} \hat{\mathbf{X}}_t - \hat{\theta}_t^2 \Bigg\{ \int_t^{\tau_1^2} \hat{\sigma}_u \hat{\mathbf{a}}_{t,\tau_1^2,\tau_2^2} \mathbf{e}_p du \\ & + \int_{\tau_1^2}^{\tau_2^2} \hat{\sigma}_u \mathbf{e}_1^\top A^{-1} \left[\exp\left\{ A(\tau_2^2 - u) \right\} - I_p \right] \mathbf{e}_p du \Bigg\} \Bigg)^2 \end{aligned} \tag{30}$$

To get an estimate of $\hat{\theta}_t^3$, $\hat{\theta}_t^2$ is substituted in the period (τ_1^2, τ_2^2) of the next equation:

$$\begin{aligned} \underset{\hat{\theta}_t^3}{\arg\min} \quad \Bigg(& F_{CAT(t,\tau_1^3,\tau_2^3)} - \int_{\tau_1^3}^{\tau_2^3} \hat{\Lambda}_u du - \hat{\mathbf{a}}_{t,\tau_1^3,\tau_2^3} \hat{\mathbf{X}}_t - \int_t^{\tau_1^2} \hat{\theta}_t^2 \hat{\sigma}_u \hat{\mathbf{a}}_{t,\tau_1^3,\tau_2^3} \mathbf{e}_p du \\ & - \int_{\tau_1^3}^{\tau_2^3} \hat{\theta}_t^3 \hat{\sigma}_u \mathbf{e}_1^\top A^{-1} \left[\exp\left\{ A(\tau_2^3 - u) \right\} - I_p \right] \mathbf{e}_p du \Bigg)^2 \end{aligned} \tag{31}$$

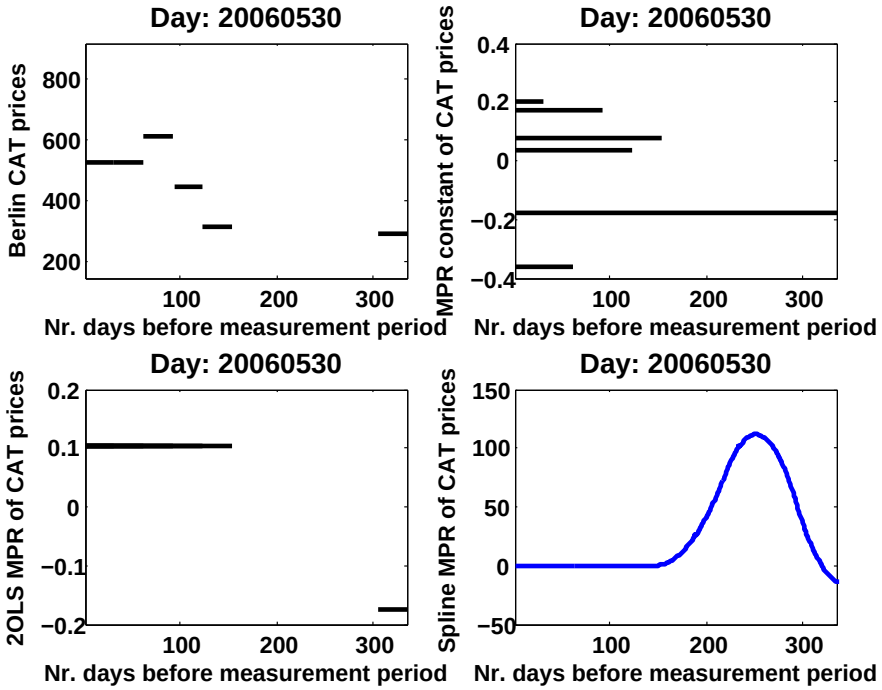

Figure 19: Prices (upper left) and MPR for Berlin CAT Futures traded on 20060530. Constant MPR for each contract per trading day (upper right), 2 constant MPR per trading day (lower left) and time dependent MPR using spline (lower right).

Then substitute $\hat{\theta}_2$ in the period (τ_1^2, τ_2^2) and $\hat{\theta}_3$ in the period (τ_1^3, τ_1^3) to estimate $\hat{\theta}_4$:

$$\begin{aligned}\underset{\hat{\theta}_t^4}{\arg\min} \quad \Bigg(\quad & F_{CAT(t,\tau_1^4,\tau_2^4)} - \int_{\tau_1^4}^{\tau_2^4} \hat{\Lambda}_u du - \hat{\mathbf{a}}_{t,\tau_1^4,\tau_2^4} \hat{\mathbf{X}}_t - \int_t^{\tau_1^2} \hat{\theta}_t^2 \hat{\sigma}_u \hat{\mathbf{a}}_{t,\tau_1^4,\tau_2^4} \mathbf{e}_p du \\ & - \int_{\tau_1^2}^{\tau_1^3} \hat{\theta}_t^3 \hat{\sigma}_u \hat{\mathbf{a}}_{t,\tau_1^4,\tau_2^4} \mathbf{e}_p du - \int_{\tau_1^4}^{\tau_2^4} \hat{\theta}_t^4 \hat{\sigma}_u \mathbf{e}_1^\top A^{-1} \left[\exp\left\{ A(\tau_2^4 - u) \right\} - I_p \right] \mathbf{e}_p du \Bigg)^2 \end{aligned} \tag{32}$$

In a similar way, the estimation of $\hat{\theta}_t^5$, $\hat{\theta}_t^6$ $\hat{\theta}_t^7$ can be obtained. The estimates of the bootstrap MPR lead to full replication of the CAT futures prices, as in the case when the MPR is constant per trading day. The relative difference between the bootstrap method and the constant MPR per trading day method $(|MPRbootstrap - MPRconstant| / M$ is equal to -1.2895e-004, while for the constant MPR, the two constant MPRs and the MPR obtained by splines the differences are equal to 6.3714, 7.4945 and 0.0232 respectively.

Figure 20 shows the box plot per CAT future contract type of the MPR estimates when this one is assummed to be constant per contract per trading day, constant per trading day (OLS), 2 constants per trading day (OLS2), Boostrap and time dependent (represented by the Spline MPR). The data includes the MPR estimates from 20060501 to 20060530. Observe that in most of cases, the median and mean of the MPR per contract $i = 2, \ldots, 7$ is negative, meaning that buyers of temperature derivatives are expecting to pay lower prices to hedge their weather risk. However, one can notice that on some days of contract 2,3,6 and 7, the MPR is positive, indicating the existance of consumers, who consider temperature derivatives as a kind of insurance.

To see how big the deviations from one estimation to another one are, we define the relative differences between estimations as the absolute value of the MPR estimation differences divided by the value of the constant MPR,

whose estimates lead to a full replication of prices. Figure 21 displays the relative differences between the estimates of the MPR from the previous subsections and the constant MPR per contract per trading day. The differences between estimations are more visible over contract type, but in all of them the relative differences from the general form of the MPR obtained from splines and the boostrap are insignificant, while for constant MPR for all types of contracts, the estimates show to have the highest relative difference.

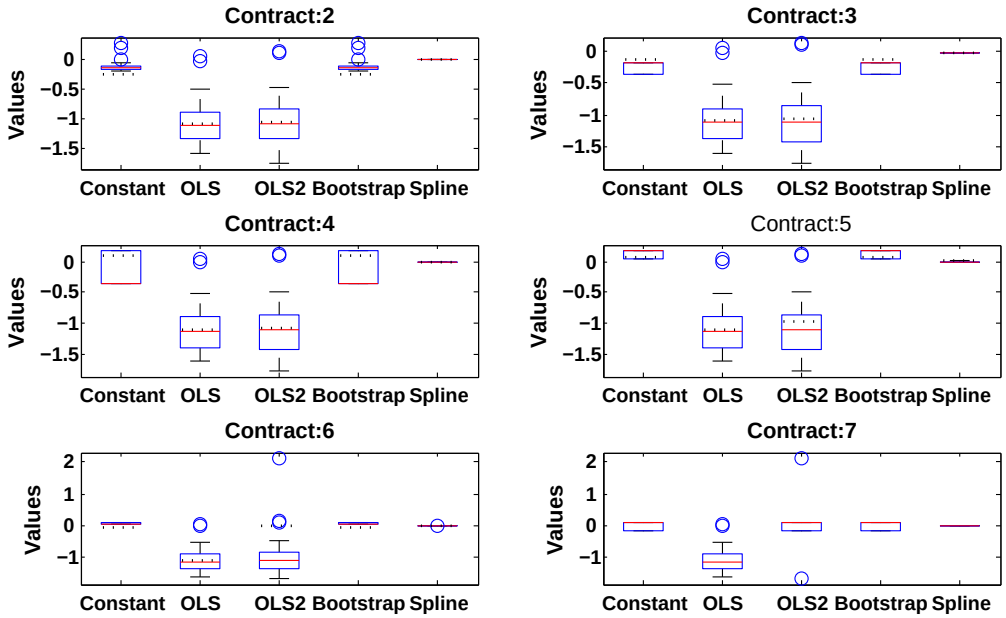

Figure 20: Box plot per CAT future contract type of the MPR estimates (20060501- 20060530) when this one is constant per contract per trading day, constant per trading day (OLS), 2 constants per trading day (OLS2), Boostrap and smooth by Spline.

4.6 Smoothing the market price of risk over time

After computing the MPR $\hat{\theta}_t$ for each of the trading days for different contracts, a smoothing of the MPR with the inverse problem points can be made to find a MPR $\hat{\theta}_u$ for every calendar day and with that one can price temperature derivative for any maturity. We performed two procedures. The first one consists on smoothing the MPR that was estimated in the previous subsection, i.e:

$$\arg\min_{f\in\mathcal{F}_j} \Sigma_{t=1}^{n} \left\{\hat{\theta}_t - f(u_t)\right\}^2 = \arg\min_{\alpha_j} \Sigma_{t=1}^{n} \left\{\hat{\theta}_t - \Sigma_{j=2}^{7}\alpha_j \Psi_j(u_t)\right\}^2 \tag{33}$$

where $\Psi_j(u_t)$ is a vector of known basis functions, α_j defines the coefficients and $u_t = t + \Delta - 1$ and n is the number of days to be smoothed. In our case $u_t = 1$ day and $\Psi_j(u_t)$ is estimated using cubic splines. Figure 22, Figure 23 and Figure 24 show the MPR smoothing for 1, 5 and 30 days of the constant MPR per contract per day (upper left), the constant MPR per day (upper right), the 2 constant MPR per day (middle left), the Bootstrap MPR (middle right) and the Spline MPR (lower left) for Berlin CAT Future traded on 20060530.

Instead of smoothing the MPR estimation in two steps, the second approach follows the estimation and smooth-

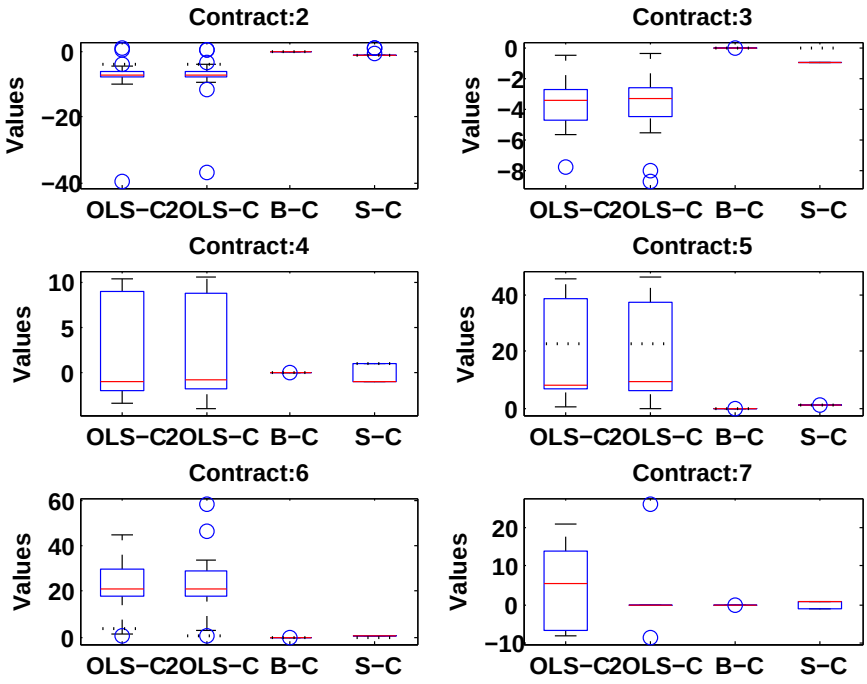

Figure 21: Box plot per CAT future contract type of the relative differences (20060501- 20060530) between MPR estimates: MPR constant per contract per trading day (C), MPR constant per trading day (OLS), 2 MPR constant per trading day (2OLS), Bootstrap MPR (B), Spline MPR (S).

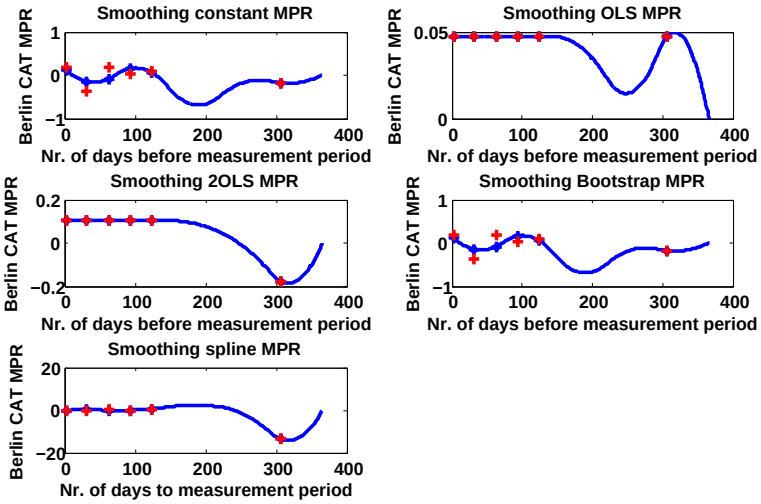

Figure 22: MPR smoothing for 1 day: the constant MPR per contract per day (upper left), the constant MPR per day (upper right), the two constant MPRs per day (middle left), the Bootstrap MPR (middle right) and the Spline MPR (lower left) for Berlin CAT Future traded on 20060530.

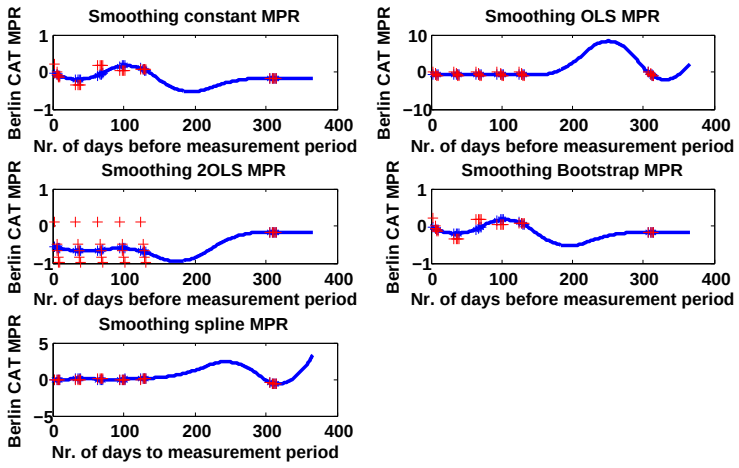

Figure 23: MPR smoothing for 5 days: the constant MPR per contract per day (upper left), the constant MPR per day (upper right), the two constant MPRs per day (middle left), the Bootstrap MPR (middle right) and the Spline MPR (lower left) for Berlin CAT Future traded on 20060530.

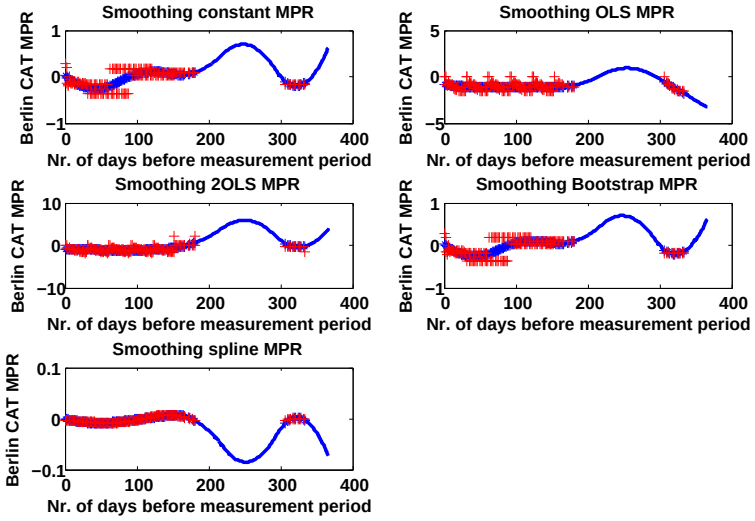

Figure 24: MPS smoothing for 30 days: the constant MPR per contract per day (upper left), the constant MPR per day (upper right), the two constant MPRs per day (middle left), the Bootstrap MPR (middle right) and the Spline MPR (lower left) for Berlin CAT Future traded on 20060530.

ing procedure in just one step. We smooth the estimation of two constant market prices of risk per trading day over several days t as:

$$\begin{aligned}\underset{\hat{\theta}_t^1,\hat{\theta}_t^2}{\arg\min}\,\Sigma_{t=1}^{n}\Sigma_{i=2}^{7} \quad \Bigg(\quad & F_{CAT(t,\tau_1^i,\tau_2^i)} - \int_{\tau_1^i}^{\tau_2^i} \hat{\Lambda}_u du - \hat{\mathbf{a}}_{t,\tau_1^i,\tau_2^i}\mathbf{X}_t \\ & - \hat{\theta}_t^1 \left\{ \int_t^{\tau_1^i} I\left(u \leq \xi\right) \hat{\sigma}_u \hat{\mathbf{a}}_{t,\tau_1^i,\tau_2^i} \mathbf{e}_p du + \int_{\tau_1^i}^{\tau_2^i} I\left(u \leq \xi\right) \hat{\sigma}_u \mathbf{e}_1^\top A^{-1} \left[\exp\left\{A(\tau_2^i - u)\right\} - I_p\right] \mathbf{e}_p du \right\} \\ & - \hat{\theta}_t^2 \left\{ \int_t^{\tau_1^i} I\left(u > \xi\right) \hat{\sigma}_u \hat{\mathbf{a}}_{t,\tau_1^i,\tau_2^i} \mathbf{e}_p du + \int_{\tau_1^i}^{\tau_2^i} I\left(u > \xi\right) \hat{\sigma}_u \mathbf{e}_1^\top A^{-1} \left[\exp\left\{A(\tau_2^i - u)\right\} - I_p\right] \mathbf{e}_p du \right\} \Bigg)^2 \end{aligned} \tag{34}$$

The estimation of the MPR in this particular case shows exactly the moment when the MPR changes from being positive to negative, indicating a kind of a seasonal structure. This temporal variation might explain the connection between temperature future prices and its deviations from spot prices based on the risk attitude of consumers and producers in the diversification process. It is interesting to see that the MPR have different signs depending on how many days are left before the measurement period starts. The MPR increases as the time to maturity of the CAT future increases. The left side of Figure 25, Figure 26 and Figure 27 show the MPR smoothing for 1, 5 and 30 days for Berlin CAT Future traded on 20060530 in two step procedures (smoothing the estimation), while the right hand side of those pictures display the smoothing and estimating procedure in one step. One can observe that both approaches diverge when the smoothing takes place over more calendar days.

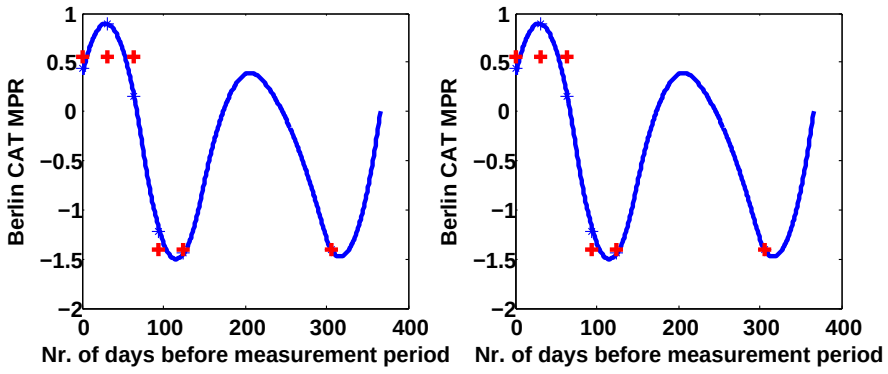

Figure 25: Smoothed MPR of Berlin CAT prices traded on 20060530 for 1 lag in 2 steps procedure (red crosses-left side) and 1 step procedure (blue line with blue crosses-right side)

4.7 Pricing CAT-HDD futures

The Chicago Mercantile exchange does not carry out trade CDD futures for Berlin, however we can use the estimates of the smoothed MPR of CAT futures in equation 24 to price CDD futures. Then from the HDD-CDD parity equation 16, one can estimate HDD futures and compare them with real data. Using the corresponding MPRs from the last section, the left hand side of Figure 28 shows the estimated CAT future prices and the

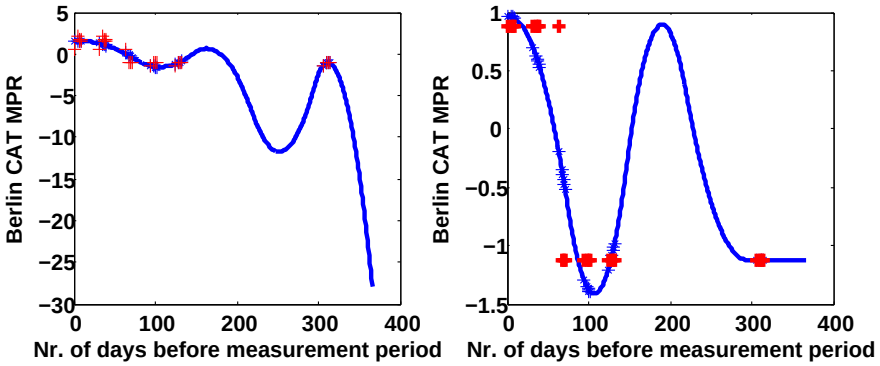

Figure 26: Smoothed MPR of Berlin CAT prices traded on 20060530 for 5 lags in 2 steps procedure (red crosses-left side) and 1 step procedure (blue line with blue crosses-right side)

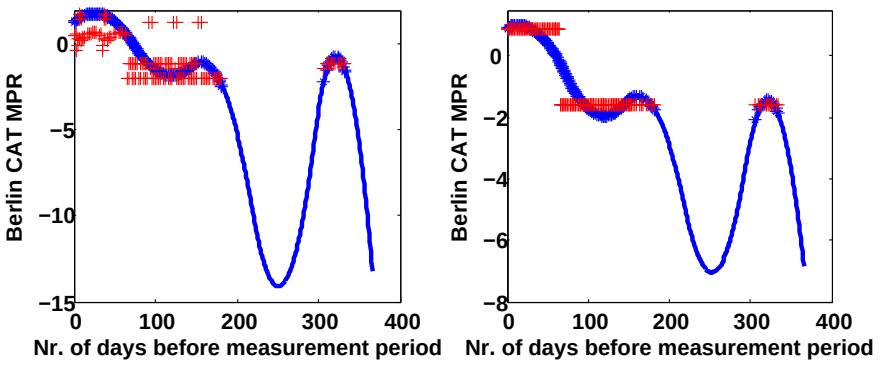

Figure 27: Smoothed MPR of Berlin CAT prices traded on 20060530 for 30 lags in 2 steps procedure (red crosses-left side) and 1 step procedure (blue line with blue crosses-right side)

real prices extracted from Bloomberg (black line) for contracts traded before the measurement period. The CAT future prices estimates replicate the Bloomberg estimates (black line) when the MPR estimate is constant per contract per trading day. The seasonality effect of the temperature is clearly reflected in the CAT future prices, showing high prices from June to August and low prices from September to April. However, pricing deviations are smoothed over time when the estimations use smoothed MPRs, as we observe in the right hand side of Figure 28. Replication of the HDD prices for Berlin are also displayed in Figure 29, when these ones are estimated from robust (left hand side) and smooth (right hand side) MPRs. The extract information does not fully replicate the reported HDD prices, indicating that there is some added value that the market use to price these kind of contracts. However we observe that a high part of the composition of the price is from the seasonal exposure. When the MPR becomes positive, there is a positive contribution to the future price which makes it larger than the estimated price.

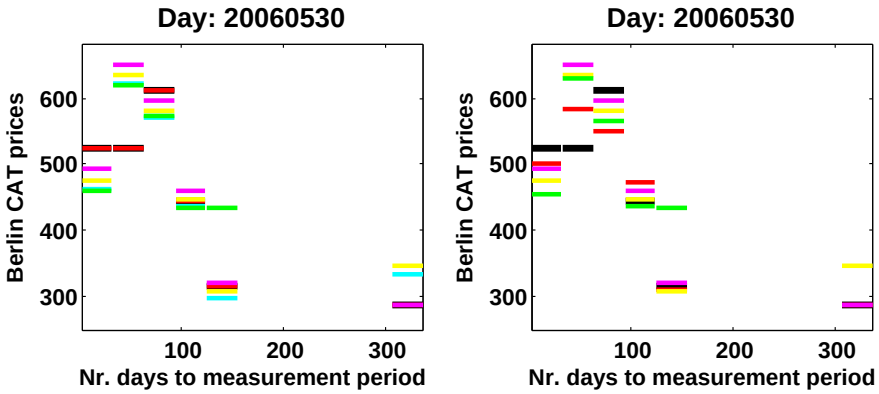

Figure 28: Right: Berlin CAT Future Prices from Bloomberg (black line) and estimated with constant MPR $\hat{\theta}_t^i$ (red line), MPR=0 (cyan line), constant MPR $\hat{\theta}_t$ (yellow line), two constant MPR $\hat{\theta}_t^1, \hat{\theta}_t^2$ (magenta line), Spline MPR (green line). Left: CAT Future Prices estimates using smoothed MPRs

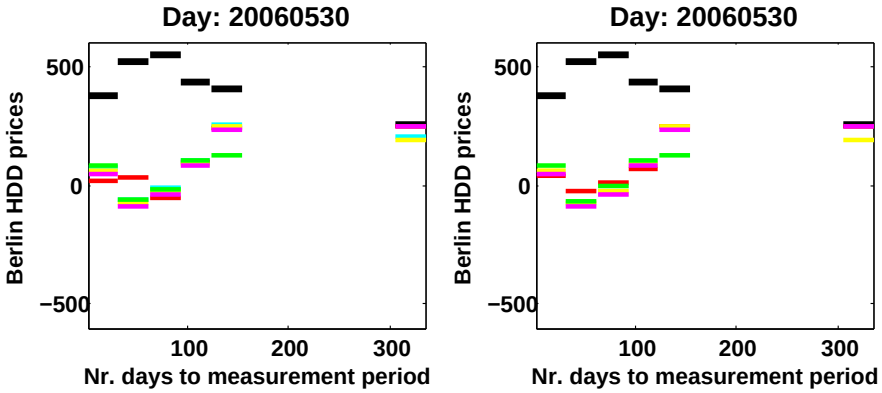

Figure 29: Right: Berlin HDD Future Prices from Bloomberg (black line) and estimated with constant MPR per contract per day (red line), MPR=0 (cyan line), constant MPR $\hat{\theta}_t$ (yellow line), two constant $\hat{\theta}_t^1, \hat{\theta}_t^2$ (magenta line), Spline MPR (green line). Left: HDD Future Prices estimates using smoothed MPR's

We also estimate the CAT futures prices for contracts traded during the measurement period. The prices also

show a seasonal pattern, confirming the idea that most of the derivative price is driven by the seasonal effect. The left hand side of Figure 30 shows the estimated CAT future prices and the real prices extracted from Bloomberg (black line) for contracts traded in and before the measurement period. The replication is almost perfect in this case, but for HDD (right hand side of the picture) deviations are emphasised.

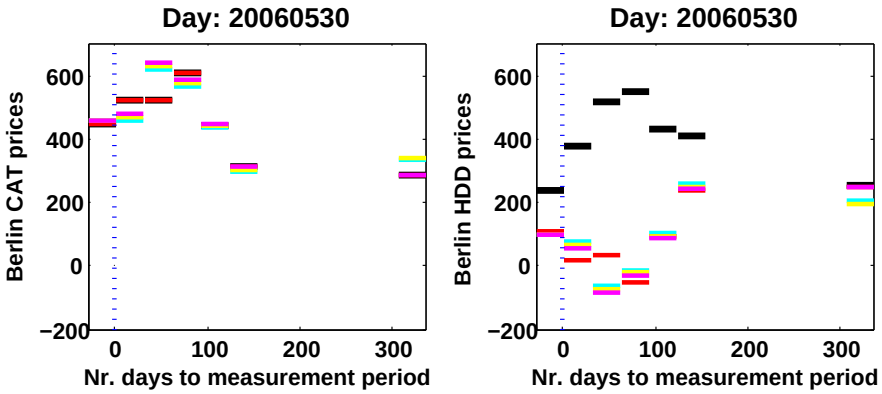

Figure 30: Berlin CAT-HDD Future Prices from Bloomberg (black line) and estimated with constant MPR per contract per day (red line), MPR=0 (cyan line), constant MPR for all contracts (yellow line), two constant MPR per day (magenta line), Spline MPR(green line)

Since CAT futures are already temperature derivatives traded in the market, we relate the seasonal effect that the MPR presents in the previous subsection with the seasonal variation of the underlying process. Figure 31 shows the behaviour of the MPR and the seasonal variation $\hat{\sigma}^2_{t+\Delta}$ for CAT future contracts with the measurement period May 2006 (Contract K6). As we expect, the relationship between the seasonal variation $\hat{\sigma}^2_{t+\Delta}$ and the MPR is more linear when the MPR $\hat{\theta}_t$ is smoothed over time (Figure 32) than when it is not $\hat{\theta}^2_t$ (Figure 33). We observe that the MPR increases as the $\hat{\sigma}^2_{t+\Delta}$ increases, i.e. the closer we are to the measurement period. This might be due to the incorporation of information from the temperature process.

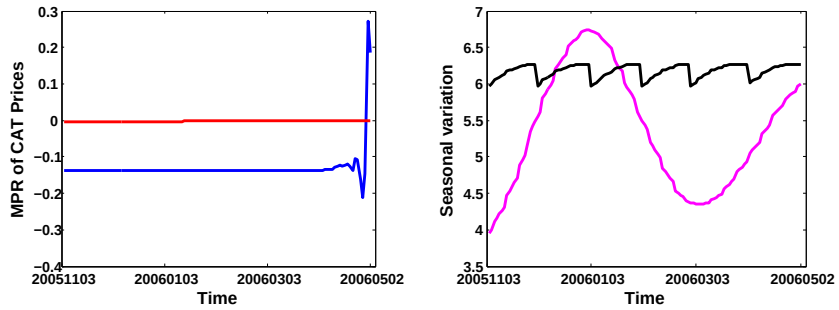

Figure 31: Left: Constant MPR $\hat{\theta}^i_t$ (blue)/smooth MPR $\hat{\theta}_t$ (red). Right: Seasonal Variation $\hat{\sigma}^2_{t+\Delta}$ (black) and $\hat{\sigma}^2_t$ (magenta) (right side) for Berlin CAT Future Prices, measurement period May 2006 (Contract K6)

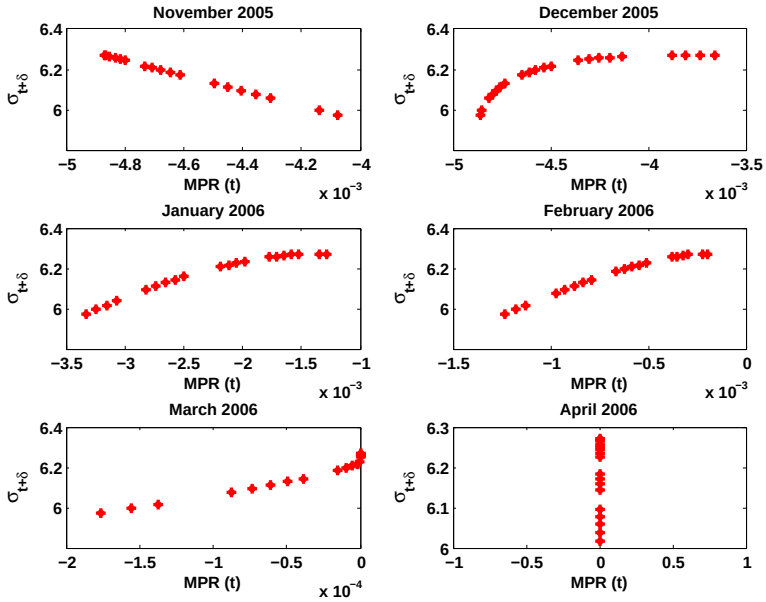

Figure 32: Seasonal Variation $\hat{\sigma}^2_{t+\Delta}$ and smoothed MPR $\hat{\theta}_t$ for Berlin CAT Future Prices 2006, measurement period May 2006 (Contract K6)

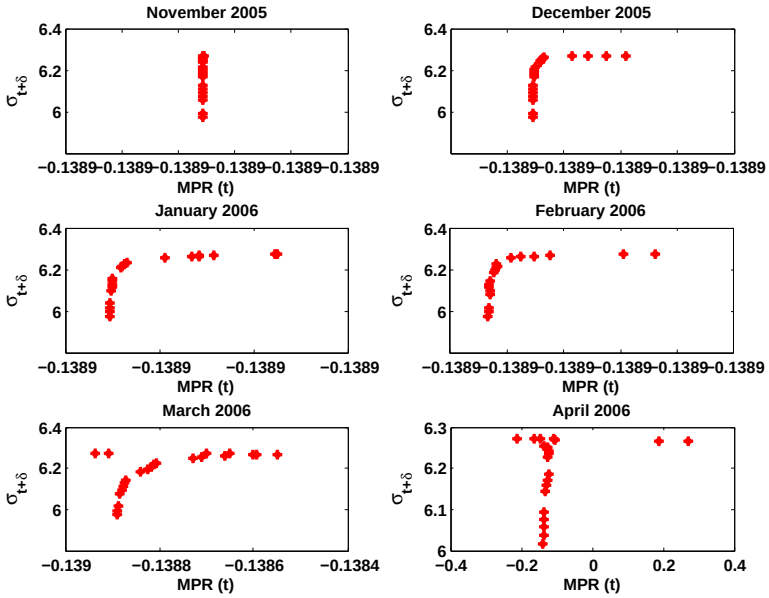

Figure 33: Seasonal Variation $\hat{\sigma}^2_{t+\Delta}$ and constant MPR $\hat{\theta}^2_t$ for Berlin CAT Future Prices, measurement period May 2006 (Contract K6)

5 Conclusion

We apply higher order continuous time autoregressive models CAR(3) with seasonal variance for modelling temperature in Berlin for more than 57 years of daily observations.

This paper also analyses the weather future products for Berlin as traded at the Chicago Mercantile Exchange (CME). We implied the market price of weather risk, which is an important issue to price non-tradable assets. We study the MPR structure, not only as a piecewise constant linear function, but also as time dependent for different contract types to obtain a full replica of real prices. By doing so, we can establish explicit relationships between the market risk premium and the MPR and explain connections between forward prices and their deviations from the spot market. We found that the MPR for cumulative temperature derivatives is different from zero and shows a seasonal structure that increases as the expiration date of the temperature future increases. The main explanation of this temporal variation is the risk attitude of consumers and producers in the diversification process and the seasonal effect of the underlying process nature. We observe a nonlinear relationship between the seasonal variation of the temperature process and the MPR, indicating that a significant portion of derivative prices could come from the different time horizont perspectives of market players to hedge weather risk.

References

(n.d.).

Alaton, P., Djehiche, B. and Stillberger, D. (2002). On modelling and pricing weather derivatives, *Appl. Math. Finance* **9(1)**: 1–20.

Barrieu, P. and El Karoui, N. (2002). Optimal design of weather derivatives, *ALGO Research* **5(1)**.

Benth, F. (2003). On arbitrage-free pricing of weather derivatives based on fractional brownian motion., *Appl. Math. Finance* **10(4)**: 303–324.

Benth, F. (2004). *Option Theory with Stochastic Analysis: An Introduction to Mathematical Finance.*, Springer Verlag, Berlin.

Benth, F., Koekebakker, S. and Saltyte Benth, J. (2007). Putting a price on temperature., *Scandinavian Journal of Statistics 2007* .

Benth, F. and Saltyte Benth, J. (2005). Stochastic modelling of temperature variations with a view towards weather derivatives., *Appl. Math. Finance* **12(1)**: 53–85.

Brody, D., Syroka, J. and Zervos, M. (2002). Dynamical pricing of weather derivatives, *Quantit. Finance* **3**: 189–198.

Campbell, S. and Diebold, F. (2005). Weather forecasting for weather derivatives, *American Stat. Assoc.* **100(469)**: 6–16.

Cao, M. and Wei, J. (2004). Weather derivatives valuation and market price of weather risk, **24(11)**: 1065–1089.

Davis, M. (2001). Pricing weather derivatives by marginal value, *Quantit. Finance* **1**: 305–308.

Dornier, F. and Querel, M. (2000). Caution to the wind, *Energy Power Risk Management* **Weather Risk Special Repor**: 30–32.

Hamisultane, H. (2007). Extracting information from the market to price the weather derivatives, *ICFAI Journal of Derivatives Markets* **4(1)**: 17–46.

Horst, U. and Mueller, M. (2007). On the spanning property of risk bonds priced by equilibrium, *Mathematics of Operation Research* **32(4)**: 784–807.

Hull, J. (2006). *Option, Future and other Derivatives*, Prentice Hall International, New Jersey.

Hung-Hsi, H., Yung-Ming, S. and Pei-Syun, L. (2008). Hdd and cdd option pricing with market price of weather risk for taiwan, *The Journal of Future Markets* **28(8)**: 790–814.

Ichihara, K. and Kunita, H. (1974). A classification of the second order degenerate elliptic operator and its probabilistic characterization, *Z. Wahrsch. Verw. Gebiete* **30**: 235–254.

Jewson, S., Brix, A. and Ziehmann, C. (2005). *Weather Derivative valuation: The Meteorological, Statistical, Financial and Mathematical Foundations.*, Cambridge University Press.

Karatzas, I. and Shreve, S. (2001). *Methods of Mathematical Finance.*, Springer Verlag, New York.

Malliavin, P. and Thalmaier, A. (2006). *Stochastic Calculus of Variations in Mathematical finance.*, Springer Verlag, Berlin, Heidelberg.

Mraoua, M. and Bari, D. (2007). Temperature stochastic modelling and weather derivatives pricing: empirical study with moroccan data., *Afrika Statistika* **2(1)**: 22–43.

Platen, E. and West, J. (2005). A fair pricing approach to weather derivatives, *Asian-Pacific Financial Markets* **11(1)**: 23–53.

Richards, T., Manfredo, M. and Sanders, D. (2004). Pricing weather derivatives, *American Journal of Agricultural Economics* **86(4)**: 1005–10017.

Turvey, C. (1999). The essentials of rainfall derivatives and insurance, *Working Paper WP99/06, Department of Agricultural Economics and Business, University of Guelph, Ontario.* .

SFB 649 Discussion Paper Series 2009

For a complete list of Discussion Papers published by the SFB 649, please visit http://sfb649.wiwi.hu-berlin.de.

001 "Implied Market Price of Weather Risk" by Wolfgang Härdle and Brenda López Cabrera, January 2009.
002 "On the Systemic Nature of Weather Risk" by Guenther Filler, Martin Odening, Ostap Okhrin and Wei Xu, January 2009.

SFB 649, Spandauer Straße 1, D-10178 Berlin
http://sfb649.wiwi.hu-berlin.de

This research was supported by the Deutsche Forschungsgemeinschaft through the SFB 649 "Economic Risk".